4-25-2023

NK cell-derived extracellular granzyme B drives epithelial ulceration during HSV-2 genital infection

Ying Shiang Lim

Aisha G Lee

Xiaoping Jiang

Jason M Scott

Adjoa Cofie

See next page for additional authors

Authors

Ying Shiang Lim, Aisha G Lee, Xiaoping Jiang, Jason M Scott, Adjoa Cofie, Sandeep Kumar, Dania Kennedy, David J Granville, and Haina Shin

Cell Reports

Article

NK cell-derived extracellular granzyme B drives epithelial ulceration during HSV-2 genital infection

Graphical abstract

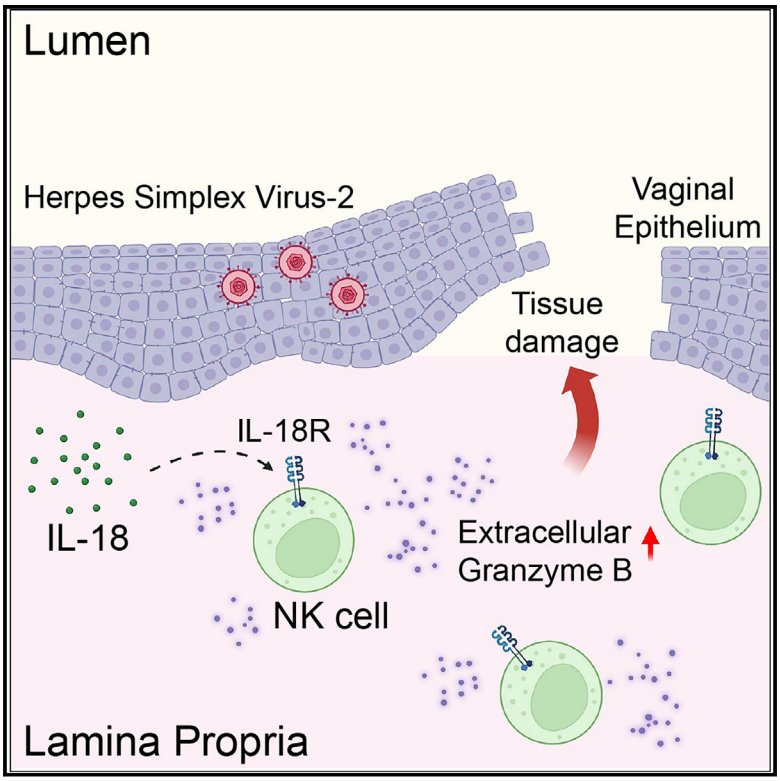

Highlights

- IL-18 induces granzyme B expression in NK cells in HSV-2 genital infections
- Granzyme B promotes tissue damage during HSV-2 genital infections
- Granzyme B-driven immunopathology is independent of perforin-1
- Therapeutic granzyme B inhibition alleviates tissue damage during HSV-2 infection

Authors

Ying Shiang Lim, Aisha G. Lee, Xiaoping Jiang, ..., Dania Kennedy, David J. Granville, Haina Shin

Correspondence

haina.shin@wustl.edu

In brief

Lim et al. show that accumulation of extracellular granzyme B produced by IL-18-stimulated NK cells is a driver of epithelial damage during vaginal infection with herpes simplex virus 2. These findings provide mechanistic insights into immunopathology during mucosal viral infection and identify a potential target for therapies to alleviate disease.

Lim et al., 2023, Cell Reports *42*, 112410
April 25, 2023
https://doi.org/10.1016/j.celrep.2023.112410

CellPress

Cell Reports

CellPress
OPEN ACCESS

Article

NK cell-derived extracellular granzyme B drives epithelial ulceration during HSV-2 genital infection

Ying Shiang Lim,[1] Aisha G. Lee,[1] Xiaoping Jiang,[1] Jason M. Scott,[1] Adjoa Cofie,[1] Sandeep Kumar,[1] Dania Kennedy,[1] David J. Granville,[2,3,4] and Haina Shin[1,5,*]

[1]Division of Infectious Disease, Department of Medicine, Washington University School of Medicine, St. Louis, MO 63110, USA
[2]International Collaboration on Repair Discoveries Centre, Vancouver Coastal Health Research Institute, Vancouver, BC V5Z 1M9, Canada
[3]Department of Pathology and Laboratory Medicine, University of British Columbia, Vancouver, BC V6T 1Z7, Canada
[4]BC Professional Firefighters' Burn and Wound Healing Research Laboratory, Vancouver, BC V5V 3P1, Canada
[5]Lead contact
*Correspondence: haina.shin@wustl.edu
https://doi.org/10.1016/j.celrep.2023.112410

SUMMARY

Genital herpes is characterized by recurrent episodes of epithelial blistering. The mechanisms causing this pathology are ill defined. Using a mouse model of vaginal herpes simplex virus 2 (HSV-2) infection, we show that interleukin-18 (IL-18) acts upon natural killer (NK) cells to promote accumulation of the serine protease granzyme B in the vagina, coinciding with vaginal epithelial ulceration. Genetic loss of granzyme B or therapeutic inhibition by a specific protease inhibitor reduces disease and restores epithelial integrity without altering viral control. Distinct effects of granzyme B and perforin deficiency on pathology indicates that granzyme B acts independent of its classic cytotoxic role. IL-18 and granzyme B are markedly elevated in human herpetic ulcers compared with non-herpetic ulcers, suggesting engagement of these pathways in HSV-infected patients. Our study reveals a role for granzyme B in destructing mucosal epithelium during HSV-2 infection, identifying a therapeutic target to augment treatment of genital herpes.

INTRODUCTION

Genital herpes is an incurable sexually transmitted infection (STI) that is caused by herpes simplex virus 2 (HSV-2) and disproportionately affects women across the globe.[1] Genital herpes is defined by recurrent episodes of genital ulcers and inflammation, and this pathology can contribute to additional adverse events, such as increased risk of acquiring other STIs, like human immunodeficiency virus (HIV),[2] particularly in areas of the world where high prevalence of HSV and HIV overlap.[3] Despite the high level of stigma and discomfort associated with the symptoms of genital herpes, little is known about the factors that cause this distinct disease. So far, the only major correlate that has been implicated in driving the pathology of symptomatic episodes is poorly controlled viral replication.[4,5] Acyclovir, the drug most commonly used to treat genital herpes, is a nucleoside analog that inactivates the viral polymerase and directly inhibits HSV replication.[6] However, while acyclovir therapy is highly effective, it does not completely suppress recurrent disease and has little impact on susceptibility to HIV infection.[7] This suggests that genital herpes pathology, particularly that which affects the vaginal barrier though which STIs enter, is not ameliorated by acyclovir therapy. Beyond the lytic effects of viral replication, the mechanisms that drive genital disease during HSV-2 infection are ill defined.

Interleukin-18 (IL-18) is a member of the IL-1 family of cytokines and is known to have pleiotropic effects in multiple cellular compartments. IL-18 was first described as a potent inducer of interferon γ (IFNγ) from lymphocytes, such as natural killer (NK) cells and T cells,[8] and therefore is best known for mediating protective type 1 immunity against several viral infections.[9–11] In support of this, studies in patients and animal models of HSV-2 vaginal infection indicate that immune responses by T cells and NK cells are largely protective and required for resolving HSV-2 replication in the vaginal mucosa in mice[12–17] and humans during recurrent disease.[18–23] During genital HSV-2 infection, IL-18 is generally considered protective because genetic deficiency of IL-18 renders mice highly susceptible to HSV-2 infection,[24] and IL-18 promotes NK cell-mediated production of IFNγ within the first couple of days of inoculation.[14,15] In contrast, our lab recently revealed opposing, time-dependent effects of IL-18, where neutralizing IL-18 during the resolution phase of infection alleviates inflammatory disease without impairing viral control in the vagina,[25] suggesting a more complex role of IL-18. Whether IL-18 is produced during recurrent HSV infection in humans and whether it exerts a protective or pathogenic effect is unknown.

Along with its impact on cytokine production, IL-18 has also been reported to enhance granzyme B expression *in vitro* and promote granzyme B-mediated cytotoxicity.[26,27] Granzyme B is a serine protease expressed in cytotoxic lymphocytes (CTLs), such as NK cells and CD8 T cells, and is best known for working in concert with perforin to facilitate the cytolytic activity of CTLs.[28–30] Directional release of granzyme B and

perforin from CTLs toward target cells such as tumors or virally infected cells triggers apoptotic pathways that ultimately result in cell death.[31–34] During viral infection, granzyme B, in conjunction with perforin, is often associated with viral control and host protection.[35–37] Perforin deficiency is dispensable for antiviral control and has little impact on secondary genital HSV-2 infection in immunized mice,[13] suggesting that cytotoxic mechanisms are dispensable for antiviral control during secondary infection. However, detection of granzyme B during recurrent episodes of genital herpes does not correlate with control of viral replication.[38] More recently, studies have demonstrated the importance of granzyme B and its proteolytic activity beyond induction of target cell death. In non-infectious disease settings, granzyme B can accumulate in the extracellular space, whether by non-specific degranulation[39] or by ''leakage'' after release of the immunological synapse between CTLs and target cells,[40,41] and drive pathology in the surrounding tissue. Granzyme B can cause blistering and epithelial denuding by directly cleaving hemidesmosomal proteins during autoinflammatory diseases of the skin[42,43] and can delay wound repair after burn injuries and in aged skin.[44,45] Whether granzyme B contributes to tissue damage in the context of viral infection is unclear.

In this study, we use a mouse model of HSV-2 infection to build on our previous findings and dissect the mechanism by which IL-18 causes pathology. We show that IL-18 acts on NK cells to induce elevated levels of extracellular granzyme B in the vagina and demonstrate a role of granzyme B in causing epithelial damage independent of perforin or changes in viral control. Importantly, the effects of granzyme B could be suppressed through therapeutic treatment of HSV-2-infected mice with VTI-1002, a granzyme B-specific protease inhibitor. IL-18 and granzyme B were markedly elevated in human herpetic ulcers compared with non-herpetic ulcers, which suggests that granzyme B may represent an immunomodulatory pathway to treat genital herpes disease by augmenting antiviral therapies.

RESULTS

IL-18 drives granzyme B expression during HSV-2 infection

In our previous study, we had shown that a high level of IL-18 in the vagina was associated with severe genital disease after vaginal HSV-2 infection in mice.[25] Local therapeutic neutralization of IL-18 after vaginal HSV-2 infection resulted in a significant reduction of disease severity.[25] Because IL-18 is best known for its modulation of lymphocyte responses,[8,46–48] and disease onset in mice coincides with robust infiltration of lymphocytes into the vagina,[16] we first examined the effector functions of T cells and NK cells after IL-18 neutralization. Female C57BL/6 mice were treated with depot medroxyprogesterone acetate (DMPA) to synchronize the estrus cycle and induce uniform susceptibility to HSV vaginal infection.[49] All mice were inoculated intravaginally (ivag) with 5,000 plaque-forming units (PFUs) of HSV-2 186 syn+. At 3, 4, and 5 days post infection (d.p.i.), mice were treated ivag with anti-IL-18 antibody or an isotype control.[25] IL-18 neutralization did not affect the total number of vaginal lymphocytes (Figure 1A). However, we found that the amount of granzyme B expressed per cell was reduced in vaginal CTLs (Figure 1B), including NK cells (Figures 1B and 1C). Thus, our data indicate that IL-18 affects the expression of cytotoxic granules in lymphocytes, especially NK cells, during HSV-2 infection.

IL-18R signaling in NK cells drives granzyme B accumulation and ulceration in the vagina

Because IL-18 appeared to have an impact on granzyme B expression in CTLs, we first examined IL-18 signaling specifically in NK cells through conditional deletion of the IL-18 receptor (IL-18R). *Il18r1*$^{fl/fl}$ mice were bred to *Ncr1*-Cre mice (Il18r conditional knockout [CKO]^{NK}) to produce mice in which IL-18R expression was ablated on group 1 innate lymphoid cells (ILC), including NK cells (Figure 2A). Vaginal HSV-2 infection of DMPA-treated Il18r CKO^{NK} mice or Cre littermate controls unexpectedly resulted in minimal differences in external disease severity (Figure 2B) and had little impact on control of viral replication in the vaginal lumen (Figure 2C) or tissue (Figure 2D), despite the expected loss of IFNγ production at 2 d.p.i. (Figure S1A).[14,15] Measurement of secreted granzyme B in the vaginal lumen at 5 d.p.i., which is the peak of granzyme B accumulation (Figure S1B), revealed that Il18r CKO^{NK} mice expressed significantly less granzyme B in the vagina relative to controls (Figure 2E). Importantly, reduction in granzyme B levels were not due to major differences in infiltration of CD4 T cell, CD8 T cells, and NK cells, which were comparable between Il18r CKO^{NK} mice and controls (Figure 2F), or changes in IL-18 levels (Figure S1C). Rather, we detected decreased expression of granzyme B specifically in IL-18R-deficient NK cells relative to controls (Figure 2G). Conventional disease scoring in murine models of HSV-2 infection typically focuses on pathology of the external genital skin and neurological signs of viral dissemination.[50] However, our cellular and molecular analyses (Figures 2C–2G) focus on the vaginal mucosa rather than the genital skin. Thus, to better understand direct relationships between host responses in the vagina and tissue damage, we chose to quantify disruptions to the vaginal epithelium.[51] To quantify mucosal pathology, we performed our analysis via histology using whole-slide imaging and measured the percentage of damaged epithelium in each mouse[51] (Figure S2). Remarkably, despite similar severity in external disease scores, Il18r CKO^{NK} mice exhibited a significant reduction in damage to the vaginal epithelium at 7 d.p.i. (Figure 2H), corresponding to decreased vaginal granzyme B levels. As we observed at 5 d.p.i., infiltration of lymphocytes into the vaginal tissue at 7 d.p.i. was comparable between Il18r CKO^{NK} mice and controls (Figure S1D). After primary vaginal infection, HSV spreads into the ganglia and then disseminates into tertiary sites such as the skin.[52–54] There was little difference in viral replication at secondary and tertiary sites of infection such as the ganglia (Figure S1E) and skin (Figure S1F), respectively, suggesting that disparity in external and internal pathology was likely not due to loss of NK cell-mediated viral restriction in the Il18r CKO^{NK} mice at distal sites of HSV-2 infection. Together, our data show that IL-18R signaling in NK cells regulates the amount of extracellular granzyme B that is recovered in the vagina during HSV-2 infection and suggest that the role of NK cells in modulating pathology may be distinct in vaginal mucosa and genital skin.

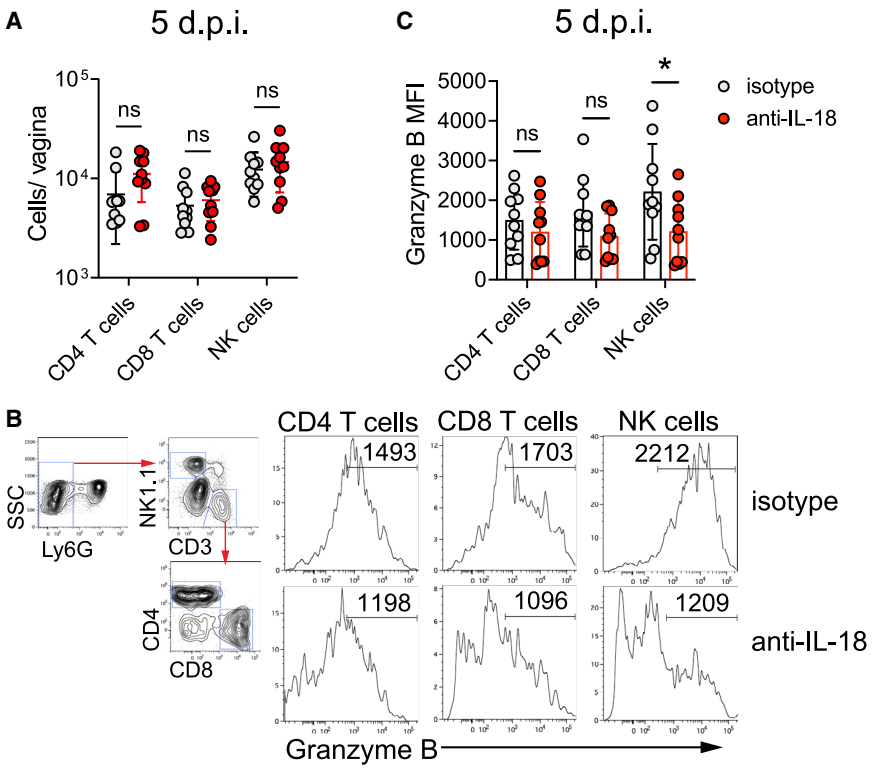

Figure 1. IL-18 drives granzyme expression *in vivo* during HSV-2 infection

DMPA-treated female WT C57BL/6 mice were infected intravaginally (ivag) with 5,000 PFUs HSV-2. Mice were treated ivag with anti-IL-18 antibody or isotype control at 3, 4, and 5 d.p.i.

(A) Graphs show the total number of each lymphocyte subset recovered from the vagina (n = 10/group).

(B) Plots show the gating strategy for analysis of vaginal lymphocytes at 5 d.p.i. Histograms show granzyme B expression in the indicated subsets. Numbers above gates show the mean fluorescence intensity (MFI) of granzyme B-expressing cells. Top row, isotype; bottom row, anti-IL-18-treated mice.

(C) MFI of granzyme B expression in each cellular subset (n = 10/group).

Data are pooled from two independent repeats. Data are represented as mean ± SD. Statistical significance was determined by one-way ANOVA with Tukey's multiple-comparisons test (A and C). *p < 0.05; ns, not significant.

IL-18R signaling in T cells does not determine disease severity during vaginal HSV-2 infection

We next wanted to confirm that the effects of IL-18 were driven by NK cells rather than T cells. To do so, we generated animals specifically lacking IL-18R1 in T cells by breeding *Il18r1*$^{fl/fl}$ × *Cd4*-Cre mice (Il18r CKO^{Tcell}) (Figure S3A). As expected, T cell-specific deletion of Il18r1 did not alleviate external genital disease (Figure S3B), as observed after IL-18 therapeutic neutralization[25] and did not alter infectious viral load in the vaginal tract (Figure S3C). Measurement of vaginal granzyme B at 5 d.p.i. showed comparable amounts between Il18r CKO^{Tcell} mice and Cre controls (Figure S3D). IFNγ levels were also equivalent between the two groups (Figure S3E), suggesting that IL-18 signaling in T cells had little *in vivo* effect on these effector molecules. Unlike NK cell-specific deletion of IL-18R, quantification of the epithelial ulceration revealed that damage to the vaginal barrier was similar between Il18r CKO^{Tcell} mice and their controls (Figure S3F). Together, the data show that IL-18R expression in T cells does not dictate disease outcomes or granzyme B accumulation in the vagina during HSV-2 infection.

Genetic deficiency of granzyme B alleviates genital tissue damage during HSV-2 infection

Our findings so far suggest a relationship between reduced granzyme B levels in the vagina and milder vaginal pathology during HSV-2 infection in mice. To determine whether granzyme B is directly required for causing barrier damage, we DMPA-treated mice genetically deficient for granzyme B (*Gzmb* knockout [KO])[55] and infected ivag with HSV-2. In contrast to Il18r CKO^{NK} mice, external disease severity was significantly reduced in *Gzmb* KO mice compared with granzyme B-sufficient littermate controls (Figure 3A). This disparity in disease was independent of differences in viral control in the vaginal lumen (Figure 3B), vaginal tissue (Figure 3C), genital skin (Figure S4A), or ganglia (Figure S4B). We also observed little difference in NK cell and T cell recruitment into the vagina at 7 d.p.i. (Figure S4C). Quantitative analysis of damage to the vaginal mucosa at 7 d.p.i. also revealed a marked reduction in epithelial ulceration in *Gzmb* KO mice compared with littermate controls (Figure 3D). In addition to directly causing damage, granzyme B has been implicated in delay of wound healing.[44,56] To distinguish between these two possibilities, we also evaluated damage of the vaginal epithelium at 5 d.p.i. At this earlier time point, while there was less mucosal damage in the *Gzmb* KO and control mice as expected, vaginal pathology in *Gzmb* KO mice was still reduced compared with controls (Figure 3E). This suggests that granzyme B accumulation at 5 d.p.i. initiates progressive epithelial denuding rather than preventing tissue repair, culminating in extensive tissue damage at 7 d.p.i. Furthermore, extracellular granzyme B can cleave hemidesmosomal components such as type XVII collagen (collagen XVII)[42,57,58] and drive pathology during non-infectious blistering diseases.[43,45] Accordingly, we found that, during HSV-2 genital infection, the expression of collagen XVII was progressively disrupted over the course of infection (Figure S5A). An increasing number of granzyme B-expressing cells could be detected in close proximity to areas of vaginal epithelial damage and disrupted collagen XVII staining (Figure S5A), and areas of vaginal epithelial ulceration exhibited a significantly greater concentration of granzyme B+ cells compared with areas of intact epithelium (Figures S5B and S5C). Importantly, *Gzmb* KO mice infected with HSV-2 displayed near-intact collagen XVII expression along the basal epithelial layer throughout the vagina, which was in stark contrast to the

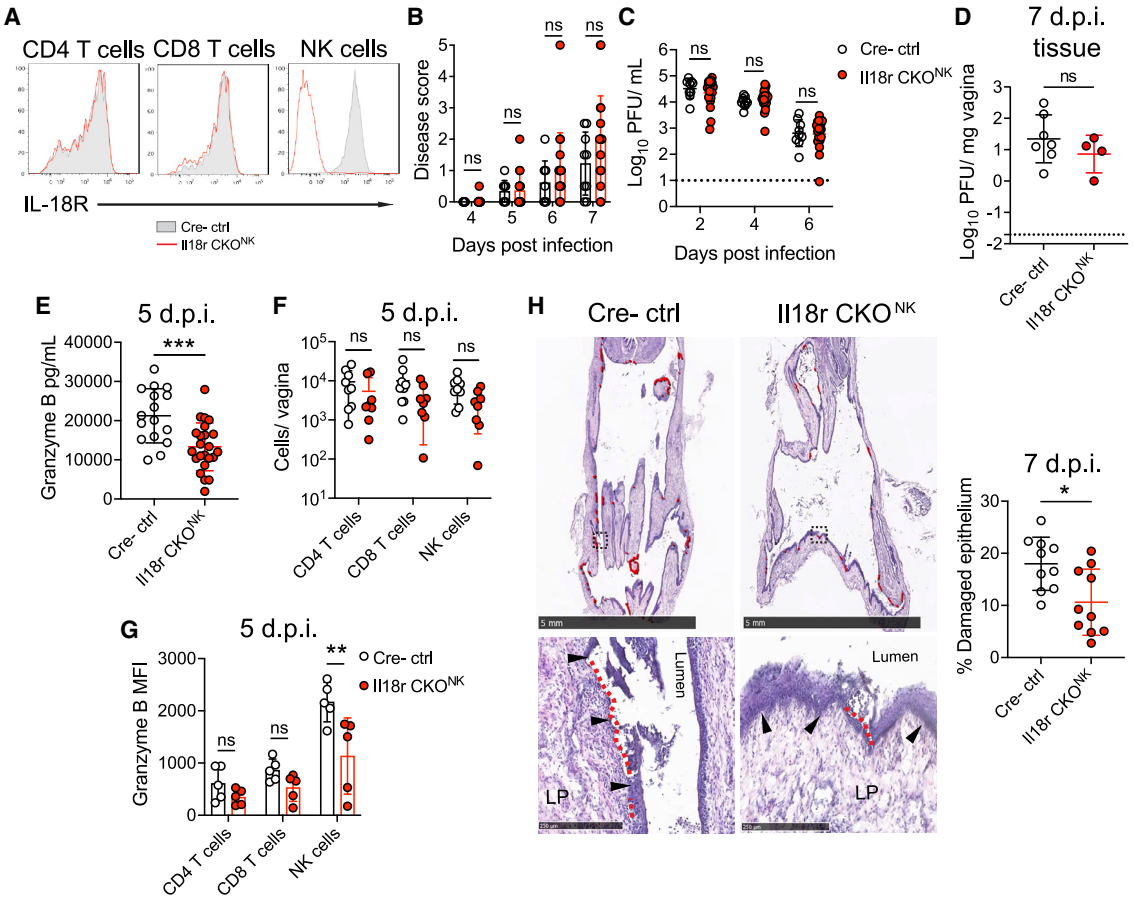

Figure 2. IL-18R signaling in conventional NK (cNK) cells drives granzyme B accumulation and ulceration in the vagina

DMPA-treated *Il18r1*$^{fl/fl}$ × *Ncr1*-Cre (Il18r CKO^{NK}) mice or Cre littermate controls were infected as described in Figure 1.

(A) Representative staining of IL-18R on the indicated vaginal cell subsets at 5 d.p.i., as analyzed by flow cytometry. Gray-shaded histograms show cells from Cre controls (ctrls), and red histograms show cells from Il18r CKO^{NK} mice.

(B) Disease scores over the first 7 d.p.i. of Cre ctrls (n = 9) or Il18r CKO^{NK} mice (n = 18).

(C and D) Infectious virus, represented as Log_{10} PFUs/mL, was determined by plaque assay of vaginal washes on the indicated days in vaginal washes (Cre ctrls, n = 9; Il18r CKO^{NK}, n = 18) (C) and in homogenized vaginal tissues at 7 d.p.i. (Cre ctrls, n = 7; Il18r CKO^{NK}, n = 4) (D).

(E) Vaginal granzyme B levels were determined by ELISA in washes at 5 d.p.i. in Cre ctrls (n = 16) or Il18r CKO^{NK} mice (n = 23).

(F and G) Graphs show the number of indicated cells types counted in the vagina (F) or MFI of granzyme B expression in the indicated cell types (G) from Cre ctrls or Il18r CKO^{NK} mice (n = 5/group) at 5 d.p.i., as determined by flow cytometry.

(H) Vaginal tissues were harvested at 7 d.p.i. for hematoxylin and eosin (H&E) staining. Top panels show examples of imaged vaginal sections. Scale bars, 5 mm. Red lines and dotted lines indicate damaged epithelium. Black dotted boxes show the magnified area in the bottom panel. Black arrows denote the basement membrane. LP, lamina propria. Bottom panel scale bars, 250 μm. The graph shows the percentage of damaged epithelium (n = 10/group, 1 section analyzed per mouse).

Data are representative of 2 independent repeats (A), pooled from 3 independent repeats (B, C, and H), 2 repeats (D), 5 repeats (E), and 4 repeats (F and G). Data in (B) are represented as median with 95% confidence interval and mean ± SD in (D)–(H). Statistical significance was determined by two-way ANOVA with Geisser-Greenhouse correction and Bonferroni's multiple-comparisons test (B), two-way ANOVA with Bonferroni's multiple-comparisons test on log-transformed values (C), Student's t test (D, E, and H), or one-way ANOVA with Tukey's multiple-comparisons test (F and G). *p < 0.05, **p < 0.01, ***p < 0.005.

discontinuous expression in littermate controls (Figure 3F). While localized areas of damage were apparent in the *Gzmb* KO mice, presumably caused by viral cytopathic effects, the pattern of collagen XVII expression was distinct from that observed in control mice (Figure 3F). Finally, granzyme B has been reported to cleave pro-IL-18 into its active form.[59] However, we found that, while vaginal granzyme B levels were absent in the *Gzmb* KO mice, as expected (Figures S4D and 3F), there was no difference in IL-18 (Figure S4E), indicating that the action of granzyme B lay downstream of IL-18. Collectively, our data reveal granzyme B as a crucial driver of immunopathology at the vaginal mucosa and genital skin during genital HSV-2, likely through destruction of barrier integrity.

Perforin deficiency does not alleviate epithelial damage in the vagina during HSV-2 infection

Given the well-established relationship between perforin and granzyme B in mediating the cytolytic activity of lymphocytes,[33,34,60]

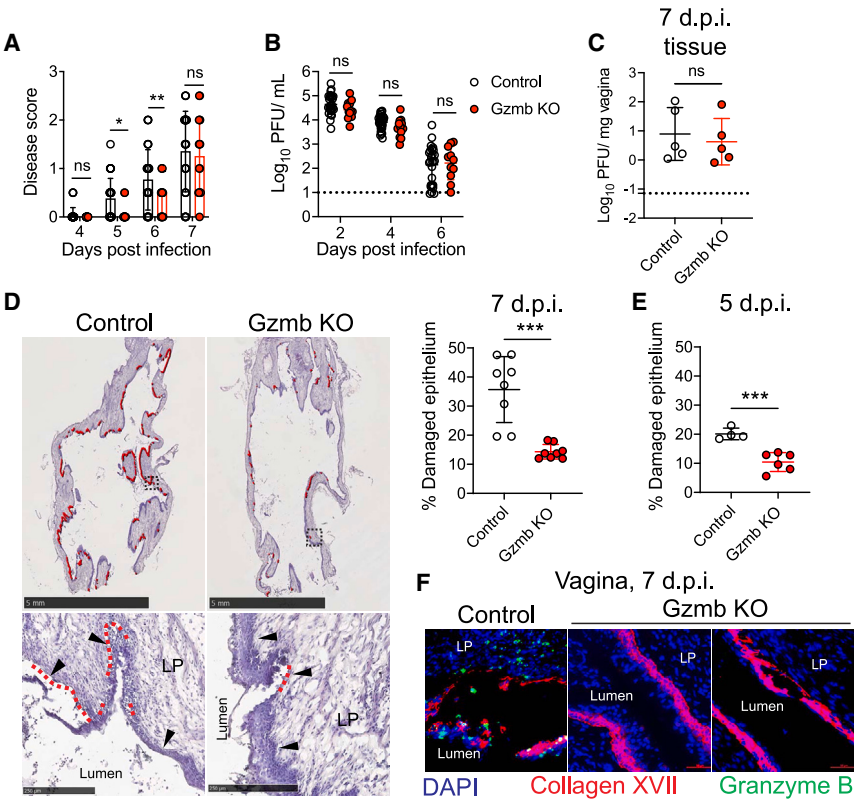

Figure 3. Genetic deficiency of granzyme B alleviates genital tissue damage without impairing viral control during HSV-2 infection

(A) Disease scores over the first 7 d.p.i. of granzyme B knockout mice (*Gzmb* KO, n = 16) or littermate granzyme B-sufficient ctrls (n = 30–32).

(B and C) Infectious viral loads, represented as Log_{10} PFUs/mL, were determined by plaque assay on vaginal washes taken on the indicated days from *Gzmb* KO (n = 12) or littermate ctrls (n = 27) (B) and homogenized vaginal tissues at 7 d.p.i. (n = 5/group) (C). Vaginal tissues were harvested at 7 d.p.i. for H&E staining. The entire vaginal epithelium was imaged, and red lines outline damaged epithelium. Scale bars, 5 mm. Black dotted boxes show the magnified area in the bottom panel. Red dotted lines indicate damaged epithelium. Black arrows denote the basement membrane. Bottom panel scale bars, 250 μm.

(D and E) The percentage of damaged epithelium was quantified at 7 d.p.i. (D) (n = 4/group, 2 independent sections analyzed per mouse) and 5 d.p.i. (E) (n = 4/group, 1–2 sections analyzed per mouse).

(F) Vaginal tissues were harvested from *Gzmb* KO and littermate ctrls at 7 d.p.i. and stained with antibodies against collagen XVII (red), granzyme B (green), and DAPI (blue). Scale bars, 50 μm.

Data are pooled from 9 independent repeats (A), 5 repeats (B), 3 repeats (C, D, and F), and 2 repeats (E). Data in (A) are represented as median with 95% confidence interval and mean ± SD in (B)–(E). Statistical significance was determined by two-way ANOVA with Geisser-Greenhouse correction and Bonferroni's multiple-comparisons test (A), two-way ANOVA with Bonferroni's multiple-comparisons test (B), or Student's t test (C–E). *p < 0.05, **p < 0.01, ***p < 0.005.

we next wanted to test whether vaginal immunopathology required the perforin-dependent, apoptosis-inducing activity of granzyme B. Unlike *Gzmb* KO mice, perforin-deficient (*Prf1* KO) mice infected vaginally with HSV-2 displayed external disease scores comparable with WT controls (Figure 4A). However, while vaginal viral burden was similar at 2 and 4 d.p.i., resolution of infection was delayed in *Prf1* KO mice compared with wild-type (WT) controls (Figures 4B and 4C). Furthermore, although vaginal granzyme B accumulation was comparable between *Prf1* KO mice and WT controls at 5 d.p.i., granzyme B levels remained elevated in *Prf1* KO mice (Figure 4D). Accordingly, we found that *Prf1* KO mice exhibited markedly more damage to the vaginal epithelium at 7 d.p.i. (Figure 4E), which was in stark contrast to external disease severity. Together, our data demonstrate that perforin and granzyme B play distinct roles in viral control and induction of tissue damage during HSV-2 infection and that the pathogenic activity of granzyme B can be uncoupled from its classic perforin-dependent cytotoxic function.

Therapeutic inhibition of granzyme B reduces genital tissue damage during HSV-2 infection

Because granzyme B ablation could reduce disease without affecting viral control, we wanted to determine whether this protease would make a feasible target for reducing mucosal disruption during genital herpes. To test this, we used VTI-1002, a gel-formulated small-molecule inhibitor that has a high degree of specificity for granzyme B enzymatic activity[44] and has been successfully used to reduce pathology in autoinflammatory diseases affecting the skin.[42,45] DMPA-treated mice were inoculated with HSV-2 and treated daily with topical VTI-1002 or a control gel from 4–6 d.p.i. through an ivag route (Figure 5A). Therapeutic inhibition of granzyme B protease activity resulted in a marked reduction of vaginal epithelial damage relative to mice receiving the control gel (Figure 5B) and did not inhibit viral control (Figure 5C). Furthermore, the distribution of collagen XVII was largely uninterrupted in VTI-1002-treated animals, similar to *Gzmb* KO mice, despite robust infiltration of cells expressing granzyme B (Figure 5D), suggesting that granzyme B protease activity in the extracellular space was responsible for cleavage of this hemidesmosomal component. We also treated HSV-2-infected *Prf1* KO mice with the granzyme B inhibitor to determine whether increased viral burden (Figures 4B and 4C) or sustained granzyme B accumulation (Figure 4D) was responsible for the extensive epithelial damage in these mice. We found that treatment with the inhibitor had no effect on viral replication or clearance (Figure 5SD). Furthermore, the granzyme B inhibitor had little impact on barrier damage (Figure S5E), suggesting that uncontrolled viral replication can also lyse epithelial cells. Although

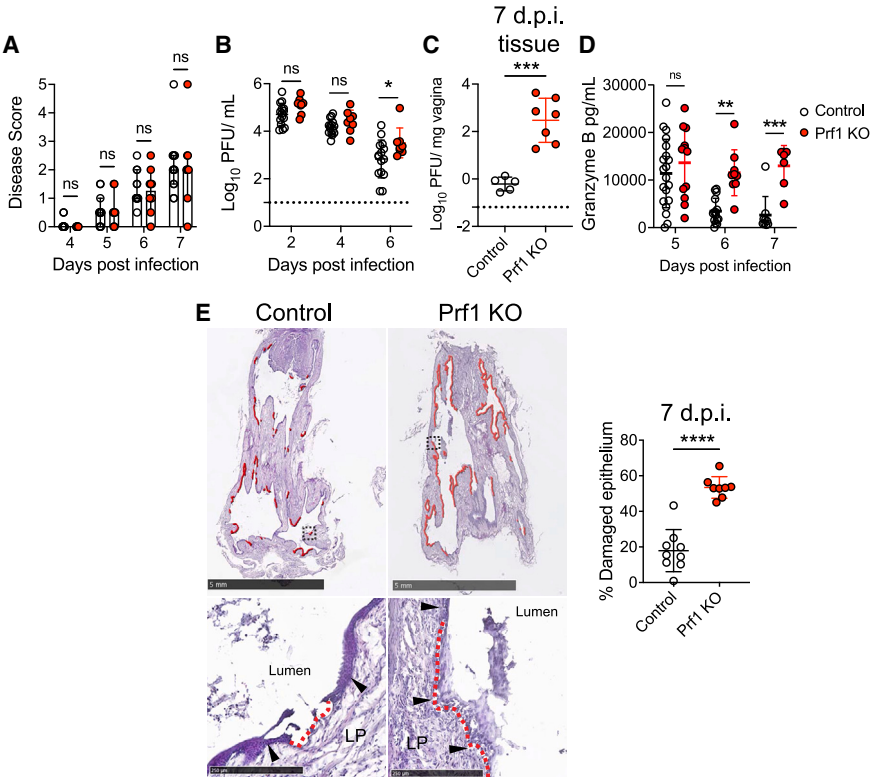

Figure 4. Perforin deficiency does not alleviate epithelial damage in the vagina during HSV-2 infection

(A) Inflammation scores over the first 7 d.p.i. of perforin-1 KO mice (*Prf1* KO; n = 10) or WT ctrls (n = 14).

(B and C) Infectious viral loads, represented as Log_{10} PFUs/mL, were determined by plaque assay on the indicated days in vaginal washes (*Prf1* KO, n = 8; WT ctrls, n = 15) (B) and in homogenized vaginal tissues at 7 d.p.i. (*Prf1* KO, n = 7; ctrls, n = 5) (C).

(D) Vaginal granzyme B levels were determined by ELISA in washes at the indicated days in *Prf1* KO mice (n = 7–13) or ctrls (n = 9–20).

(E) Vaginal tissues were harvested at 7 d.p.i. for H&E staining. The entire vaginal epithelium was imaged, and red lines outline damaged epithelium. Scale bars, 5 mm. Black dotted boxes show the magnified area in the bottom panel. Red dotted lines indicate damaged epithelium. Black arrows denote the basement membrane. Bottom panel scale bars, 250 μm. The percentage of damaged epithelium was quantified at 7 d.p.i. (*Prf1* KO, n = 4, 2 independent sections quantified per mouse; ctrls, n = 9, 1 independent section quantified per mouse).

Data are pooled from 5 independent repeats (A, B, and D) and 2 repeats (C and E). Data in (A) are represented as median with 95% confidence interval and mean ± SD in (B)–(E). Statistical significance was determined by two-way ANOVA with Geisser-Greenhouse correction and Bonferroni's multiple-comparisons test (A), two-way ANOVA with Bonferroni's multiple-comparisons test (B and D), or Student's t test (C and E). *p < 0.05, **p < 0.01,***p < 0.005, ****p < 0.0001.

granzyme B has been evaluated previously in recurrent genital herpes in women,[19,38] whether IL-18 is also produced during human infection is unclear. To determine whether IL-18 and granzyme B could be concurrently detected during HSV-induced pathology in humans, we measured both analytes in swabs taken from patients suffering from ulcers of unknown etiology. We found that IL-18 (Figure 5E) and granzyme B (Figure 5F) were markedly upregulated in ulcers that had been PCR confirmed as HSV positive. Furthermore, we found a significant correlation between the magnitude of IL-18 and granzyme B protein in the ulcers, suggesting that production and secretion of these molecules may be related (Figure 5G). Collectively, our data show that granzyme B could be therapeutically targeted to reduce the inflammation and tissue damage associated with genital herpes without impairing crucial antiviral control mechanisms and may represent a novel target for therapeutics aimed at reducing clinical signs of disease and barrier damage.

DISCUSSION

In this study, we evaluated cellular and molecular drivers of tissue pathology using an animal model for a clinically important disease, genital herpes. We had previously identified IL-18 as a key component of the immunopathogenic response against vaginal HSV-2 infection in mice. Here, we found that IL-18R signaling specifically in NK cells led to accumulation of granzyme B in the vaginal tissue and lumen, likely through regulation of granzyme B expression and degranulation, and was associated with increased epithelial ulceration in the vagina but not genital skin. Granzyme B, but not perforin, was required for tissue damage of vagina and skin because deletion of granzyme B reduced pathology at both sites without compromising lymphocyte recruitment and viral control. Our findings suggest that the tissue damage caused by granzyme B is likely not due to the classic cytotoxic activity of granzyme B and perforin but rather due to cleavage of hemidesmosomal proteins that help to anchor the epithelium to the basement membrane. Moreover, topical inhibition of granzyme B using a specific protease inhibitor in the vaginal lumen also reduced tissue damage, demonstrating the therapeutic potential of targeting granzyme B. Importantly, we found that IL-18 and granzyme B were coordinately upregulated in swab samples taken from patients with herpetic ulcers compared with non-herpetic ulcers, suggesting that the pathogenic mechanisms we delineated in mice may also be active during human genital herpes disease. Together, our results reveal key host-derived mediators of tissue damage using a model of vaginal HSV-2 infection and identify a potential therapeutic target for alleviating genital herpes disease.

In the context of HSV infection and genital herpes, IL-18 and NK cells have been shown to confer protection by promoting innate antiviral responses[61–64] through production of antiviral cytokines such as IFNγ[14,24] and recruitment of other immune cells.[65] Importantly, previous studies have shown that IL-18 can directly induce IFNγ production from NK cells during the first couple of days of genital HSV-2 infection,[14] which is supported by our own data. However, our study suggests that continued

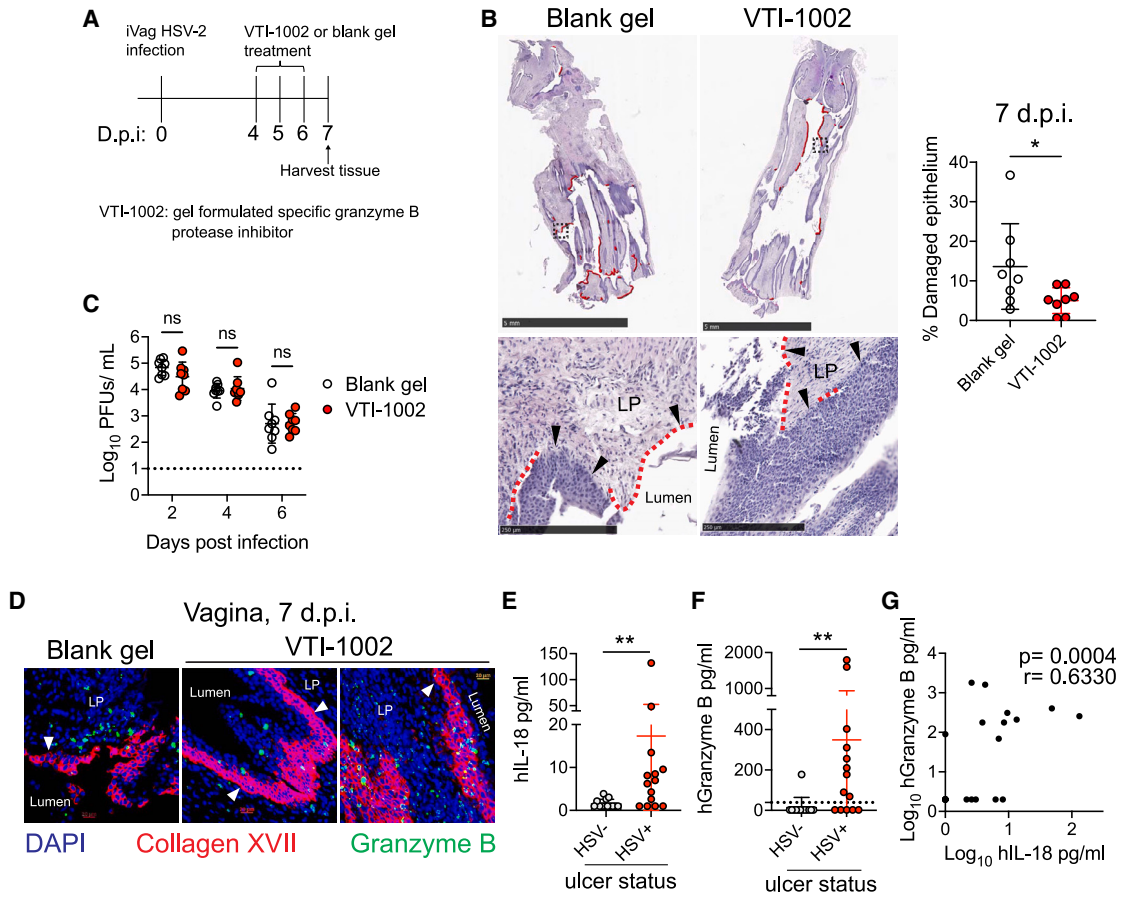

Figure 5. Therapeutic inhibition of granzyme B alleviates genital tissue damage

(A) Experimental schematic. Female WT C57BL/6 mice were infected as stated in Figure 1. Mice were treated ivag with VTI-1002 or blank gel ctrl at 4, 5, and 6 d.p.i. Tissues were harvested at 7 d.p.i. for analysis.

(B) Vaginal tissues were harvested at 7d.p.i. for H&E staining. The entire vaginal epithelium was imaged, and red lines outline damaged epithelium. Black dotted boxes show the magnified area in the bottom panel. Red dotted lines indicate damaged epithelium. Black arrows denote the basement membrane. Bottom panel scale bars, 250 μm. The percentage of damaged epithelium was quantified at 7 d.p.i. (n = 8/group, 1 independent section analyzed per mouse).

(C) Infectious virus was determined by plaque assay on vaginal washes taken on the indicated days (n = 8/group).

(D) Vaginal tissues were harvested at 7 d.p.i. and stained with antibodies against collagen XVII (red), granzyme B (green), and DAPI (blue) for detection of cell nuclei. White arrows show the basement membrane. Scale bars, 20 μm.

(E and F) Swab samples were taken from HSV− and HSV+ genital ulcers in humans and sampled by ELISA for human IL-18 (hIL-18) (HSV− ulcers, n = 13; HSV+ ulcers, n = 14) (E) and human granzyme B (hGranzymeB) (HSV− ulcers, n = 7; HSV+ ulcers, n = 13; HSV+ ulcers, n = 14) (F).

(G) Correlation of Log_{10} hGranzymeB levels in human genital ulcers on the y axis with Log_{10} hIL-18 levels on the x axis (n = 27/group).

Data are pooled from 2 independent repeats (A–D). Data are represented as mean ± SD (B, C, E, and F). Statistical significance was determined by Student's t test (B, E, and F), two-way ANOVA with Bonferroni's multiple-comparisons (C), and Pearson correlation (G). *$p < 0.05$, **$p < 0.01$.

IL-18 signaling in NK cells also drives production of pathogenic granzyme B at 5 d.p.i. within the vagina, highlighting the differential temporal outcomes of the NK cell-IL-18 axis during genital HSV-2. Furthermore, assessment of mucosal (internal) and skin (external) pathology in our study indicates that IL-18 signaling may differentially regulate NK cell activity in discrete tissue compartments. External disease scores between Il18r CKO^{NK} mice and controls were comparable, which was unexpected given the reduction of pathology in the vaginal mucosa of Il18r CKO^{NK} mice. Dissemination of HSV, which is a highly lytic virus, to tertiary tissue sites such as the skin depends on a neuronal route of spread,[52,66,67] and IL-18 and NK cells have been implicated in restricting HSV replication in the nervous system.[14,24,64] However, the severe external pathology of Il18r CKO^{NK} mice was not due to increased HSV-2 dissemination and virus-mediated damage because viral burden in the peripheral nervous tissue, central nervous tissue, and genital skin itself was similar between Il18r CKO^{NK} mice and controls. Although we did not directly measure granzyme B accumulation in the genital skin, our current studies with Gzmb KO mice and previous studies neutralizing IL-18[25] suggest that these two molecules are important for the progression of external disease. Because IL-18R signaling in NK cells appeared to be dispensable in the onset of external genital disease, it is possible that IL-18 may be acting through a different cellular compartment in the genital skin, where external disease is measured. Beyond its role in regulating

lymphocyte function, IL-18 can exert pleiotropic effects in non-hematopoietic compartments such as the gut epithelium, and more recent studies have described the impact of IL-18 on the maintenance of mucosal barrier integrity.[68,69] Keratinocytes have been shown to be able to express granzyme B upon exposure to damaging perturbations,[70,71] which raises the possibility that IL-18 may induce a non-conventional source of granzyme B to drive external genital pathology. Additionally, while protective roles of memory T cells have been extensively studied during recurrent genital herpes infection,[72] the functional role of NK cells in the context of recurrent episodes is not well understood.

Beyond its classic, perforin-dependent cytolytic activity, more recent studies have shed light on non-classical roles of granzyme B in the pathology of non-infectious and infectious diseases. As demonstrated in human and animal studies, extracellular granzyme B accumulates at lesional sites of autoimmune blistering pemphigoid diseases (PDs), such as epidermolysis bullosa acquisita (EBA) and bullous pemphigoid.[42,43] Previous studies have shown that granzyme B is able to mediate the proteolytic degradation of hemidesmosomal proteins, including type VII and type XVII collagen, and β4 and α6 integrin at the basement membrane. Furthermore, granzyme B works synergistically with neutrophil elastase (NE) to enhance proteolysis of α6 integrin during EBA.[42,43] In our model of HSV-2 infection, the later stages of external disease at 7 d.p.i. appear to progress independent of granzyme B, which indicates potential roles of other host molecules in promoting pathology. Our previous work had demonstrated a clear role of neutrophils in exacerbating disease severity in the genital skin. Whether a neutrophil-derived protease such as NE coordinates with granzyme B to drive this external pathology remains an open question. In the context of infection, lymphocyte-derived granzyme B expression has also been proposed to drive severe cutaneous leishmaniasis lesions, notably through modulation of the inflammatory cytokine environment.[73,74] While we did not observe any differences in the levels of key inflammatory cytokines such as IL-18 in the absence of granzyme B, it is possible that granzyme B may dictate disease severity by modulating the levels of other cytokines that promote pathology. Alongside the evidence that granzyme B actively causes tissue damage, studies examining wound repair after burn injury suggest that granzyme B may also inhibit subsequent tissue repair through cleavage of extracellular matrix (ECM) proteins such as decorin.[45,56,75] While our study suggests that accumulation of granzyme B directly causes epithelial ulceration during the first week after infection, whether granzyme B also regulates tissue repair after clearance of infection is unknown. Although we were unable to directly address this question in the current study because of use of a WT strain of HSV-2 that is lethal in mice, we will evaluate whether extracellular granzyme B also affects mucosal repair after infection in future studies.

Although the classic activities of granzyme B and perforin have considerable overlap,[33,34,60] our study reveals that very distinct outcomes in vaginal pathology in the context of perforin deficiency do not mimic that of granzyme B deficiency. In stark contrast to granzyme B-deficient mice, loss of perforin led to a significant increase in vaginal pathology compared with WT controls, suggesting an immunopathogenic role of perforin, as observed in ocular HSV infections.[76] Approximately one-third of degranulated granzyme B escapes into the immunological synapse and extracellular milieu.[40] Additionally, perforin deficiency in mice can also prolong immune synapse formation, leading to elevated secretion of inflammatory mediators from CTLs.[41] Perforin deficiency could thus impede intracellular delivery, leading to the observed increased vaginal granzyme B and associated heightened tissue damage. Unlike granzyme B, the role of perforin is thought to be limited to induction of CTL-mediated cytolysis.[77] While cytotoxic activity is not necessary for controlling viral replication during the early phase of HSV infection, it may be important for viral clearance.[78,79] Although viral shedding was similar between WT and perforin-deficient mice through the first 4 days of infection, genetic ablation of perforin delayed viral clearance at later time points,[80] leading to enhanced HSV-dependent cytopathic effects and greater epithelial destruction. Furthermore, our data suggest that other granzymes or cytotoxic granules may be able to compensate for the loss of granzyme B and mediate the required cytotoxic activity to promote viral clearance. While granzyme B is likely the most thoroughly studied of the cytotoxic granules, other granzymes, such as granzymes A, H, M, and K, have also been reported to be important for antiviral control through cytotoxic and non-cytotoxic mechanisms.[81–83] Additional studies will be required to determine whether these granzymes play a similar role during HSV-2 vaginal infection.

While acyclovir therapy can reduce disease severity and recurrence rates of genital herpes in patients, likely by accelerating viral control and preventing initiation of damaging host responses, acyclovir has no apparent impact on other adverse events associated with genital herpes, such as increased risk of HIV acquisition.[7] While the reason for this increased risk is unclear, one potential hypothesis that has been put forth is that genital herpes compromises vaginal barrier function, which may increase viral access to HIV-trophic target cells in the lamina propria.[3] Clinical signs of genital herpes disease in patients as well as in animal models of infection is usually evaluated by formation of ulcers on the genital skin. However, pathology at the vaginal barrier is less well defined. While HSV replication is an important component of genital herpes disease, the inability of acyclovir to reduce susceptibility to HIV, combined with the findings of our study, suggests that damage of the vaginal mucosa may be primarily driven by inflammatory host pathways that, when engaged, can continue to degrade barrier function even after viral replication is controlled. Simultaneous detection of IL-18 and granzyme B in patients with herpetic ulcers suggest that the host inflammatory pathways we identified in mice may also be active during human disease. Because inhibition of IL-18[25] or granzyme B had little impact on viral control, these molecules could be targeted in conjunction with acyclovir to fully eliminate disease and reduce adverse events that cannot be controlled with antiviral drugs alone. Beyond genital herpes, the immunopathogenic mechanisms we described here may induce tissue damage in other mucosal surfaces or tissues during other infections. More recently, elevated levels of IL-18 have been shown to correlate with severe disease in severe acute respiratory syndrome coronavirus 2 (SARS-CoV-2)-infected patients during the ongoing COVID-19 pandemic,[84–86] suggesting that IL-18

may also contribute to pathology during mucosal viral infection through an unknown mechanism. In the ongoing SARS-CoV-2 pandemic, increased granzyme B expression in hyperactivated cytotoxic T cells and NK cell subsets is associated with severe manifestations of coronavirus disease 2019 (COVID-19),[87–89] indicating that inhibition of IL-18 or granzyme B could be ideal for more targeted therapies aimed at modulating damaging host responses.

Limitations of the study

This study focused on how pathology can be induced by the immune system, specifically by granzyme B as a downstream effector of IL-18, during primary genital HSV-2 infection. Our studies were performed with a widely used model of vaginal HSV-2 infection. However, because of the complex nature of tissue pathology, which was our primary readout, we acknowledge that there is variation in the extent of disease observed from study to study. We speculate that this may likely be due to factors outside of our control (in-house-bred vs. vendor-purchased mice, housing in different animal rooms, slight variations in genetic background, etc.). We also acknowledge that there is uneven distribution of data points between the controls and experimental groups and that our figures show pooled data from an unusually large number of replicate experiments. Because of our insistence on using littermate controls and inoculating all mice at similar ages, litters were infected as they were produced, regardless of litter size, resulting in pooling of many independent experiments. Furthermore, the representation of expected genotypes in these litters was often lopsided; this was a feature of animal husbandry that was unfortunately out of our control.

Finally, our study focuses on host-mediated disease during primary HSV-2 infection. Technical limitations of this model, including the requirement of DMPA, restrict our findings to one stage of the murine estrus cycle. Considering the impact of sex hormones on antiviral host responses,[16] it is unclear whether our findings apply to other stages of the sex hormone cycle. Other differentiating factors, including vaginal microbiome composition and vaginal pH, could also affect translation of our findings from mice to humans. In humans, clinical recurrent disease manifests during reactivation of latent virus. The presence of tissue-resident memory T cells and antiviral control exerted could potentially alter the inflammatory microenvironment and augment the mechanisms involved in balancing immunopathology and protection. Unfortunately, murine models of recurrent disease are currently unavailable. Thus, future studies should include other rodent models in which recurrent disease does occur, such as guinea pigs, and ideally, these pathways should be examined in patients with genital herpes.

STAR★METHODS

Detailed methods are provided in the online version of this paper and include the following:

SUPPLEMENTAL INFORMATION

Supplemental information can be found online at https://doi.org/10.1016/j.celrep.2023.112410.

ACKNOWLEDGMENTS

We thank Dr. Michael Diamond and Dr. Chyi-Song Hsieh for comments and suggestions on the manuscript, Dr. Wandy Beatty for technical assistance with our microscopy studies, and Dr. Neil Anderson for assistance with obtaining the human samples used in this study. Funding support for this work is provided by the NIH (1R01AI134962-01A1 to H.S.). Y.S.L. is supported by funding from the Agency for Science, Technology, and Research (A*STAR, Singapore, Singapore). A.G.L. is supported by funding from an NIH F30 fellowship (1F30 AI161309-01A1). This work was also supported by the Hope Center Alafi Neuroimaging Lab and a P30 Neuroscience Blueprint Interdisciplinary Center Core award to Washington University (P30 NS057105). The graphical abstract was created with BioRender.

AUTHOR CONTRIBUTIONS

Y.S.L., A.G.L., S.K., X.J., J.M.S., A.C., and H.S. designed and conducted experiments, acquired data, and analyzed data. D.J.G. aided in the design of experiments. Y.S.L., D.K., and H.S. analyzed data. H.S. and Y.S.L. wrote the manuscript, and all authors edited the final version of the paper.

DECLARATION OF INTERESTS

D.J.G. is a co-founder and serves as the Chief Scientific Officer of viDA Therapeutics, which developed VTI-1002, the granzyme B inhibitor used in this study.

INCLUSION AND DIVERSITY

We support inclusive, diverse, and equitable conduct of research.

Received: October 26, 2022
Revised: January 25, 2023
Accepted: April 4, 2023
Published: April 17, 2023

REFERENCES

1. McQuillan, G., and Paulose-Ram, R. (2018). Prevalence of Herpes Simplex Virus Type 1 and Type 2 in Persons Aged 14–49 (United States, 2015–2016), p. 8.
2. Looker, K.J., Elmes, J.A.R., Gottlieb, S.L., Schiffer, J.T., Vickerman, P., Turner, K.M.E., and Boily, M.-C. (2017). Effect of HSV-2 infection on subsequent HIV acquisition: an updated systematic review and meta-analysis. Lancet Infect. Dis. *17*, 1303–1316. https://doi.org/10.1016/S1473-3099(17)30405-X.
3. Looker, K.J., Welton, N.J., Sabin, K.M., Dalal, S., Vickerman, P., Turner, K.M.E., Boily, M.-C., and Gottlieb, S.L. (2020). Global and regional estimates of the contribution of herpes simplex virus type 2 infection to HIV incidence: a population attributable fraction analysis using published epidemiological data. Lancet Infect. Dis. *20*, 240–249. https://doi.org/10.1016/S1473-3099(19)30470-0.
4. Schiffer, J.T., Abu-Raddad, L., Mark, K.E., Zhu, J., Selke, S., Magaret, A., Wald, A., and Corey, L. (2009). Frequent release of low amounts of herpes simplex virus from neurons: results of a mathematical model. Sci. Transl. Med. *1*, 7ra16, 7ra16.. https://doi.org/10.1126/scitranslmed.3000193
5. Schiffer, J.T., Wald, A., Selke, S., Corey, L., and Magaret, A. (2011). The kinetics of mucosal herpes simplex virus–2 infection in humans: evidence for rapid viral-host interactions. J. Infect. Dis. *204*, 554–561. https://doi.org/10.1093/infdis/jir314.
6. Elion, G.B. (1982). Mechanism of action and selectivity of acyclovir. Am. J. Med. *73*, 7–13. https://doi.org/10.1016/0002-9343(82)90055-9.
7. Celum, C., Wald, A., Lingappa, J.R., Magaret, A.S., Wang, R.S., Mugo, N., Mujugira, A., Baeten, J.M., Mullins, J.I., Hughes, J.P., et al. (2010). Acyclovir and transmission of HIV-1 from persons infected with HIV-1 and HSV-2. N. Engl. J. Med. *362*, 427–439. https://doi.org/10.1056/NEJMoa0904849.
8. Okamura, H., Tsutsi, H., Komatsu, T., Yutsudo, M., Hakura, A., Tanimoto, T., Torigoe, K., Okura, T., Nukada, Y., Hattori, K., et al. (1995). Cloning of a new cytokine that induces IFN-γ production by T cells. Nature *378*, 88–91. https://doi.org/10.1038/378088a0.
9. Ingram, J.T., Yi, J.S., and Zajac, A.J. (2011). Exhausted CD8 T cells downregulate the IL-18 receptor and become unresponsive to inflammatory cytokines and bacterial Co-infections. PLoS Pathog. *7*, e1002273. https://doi.org/10.1371/journal.ppat.1002273.
10. Liu, B., Mori, I., Hossain, M.J., Dong, L., Takeda, K., and Kimura, Y. (2004). Interleukin-18 improves the early defence system against influenza virus infection by augmenting natural killer cell-mediated cytotoxicity. J. Gen. Virol. *85*, 423–428. https://doi.org/10.1099/vir.0.19596-0.
11. Zalinger, Z.B., Elliott, R., and Weiss, S.R. (2017). Role of the inflammasome-related cytokines Il-1 and Il-18 during infection with murine coronavirus. J. Neurovirol. *23*, 845–854. https://doi.org/10.1007/s13365-017-0574-4.
12. Abdul-Careem, M.F., Lee, A.J., Pek, E.A., Gill, N., Gillgrass, A.E., Chew, M.V., Reid, S., and Ashkar, A.A. (2012). Genital HSV-2 infection induces short-term NK cell memory. PLoS One *7*, e32821. https://doi.org/10.1371/journal.pone.0032821.
13. Iijima, N., Linehan, M.M., Zamora, M., Butkus, D., Dunn, R., Kehry, M.R., Laufer, T.M., and Iwasaki, A. (2008). Dendritic cells and B cells maximize mucosal Th1 memory response to herpes simplex virus. J. Exp. Med. *205*, 3041–3052. https://doi.org/10.1084/jem.20082039.
14. Lee, A.J., Chen, B., Chew, M.V., Barra, N.G., Shenouda, M.M., Nham, T., van Rooijen, N., Jordana, M., Mossman, K.L., Schreiber, R.D., et al. (2017). Inflammatory monocytes require type I interferon receptor signaling to activate NK cells via IL-18 during a mucosal viral infection. J. Exp. Med. *214*, 1153–1167. https://doi.org/10.1084/jem.20160880.
15. Milligan, G.N., and Bernstein, D.I. (1997). Interferon-γ enhances resolution of herpes simplex virus type 2 infection of the murine genital tract. Virology *229*, 259–268. https://doi.org/10.1006/viro.1997.8441.
16. Nakanishi, Y., Lu, B., Gerard, C., and Iwasaki, A. (2009). CD8 + T lymphocyte mobilization to virus-infected tissue requires CD4 + T-cell help. Nature *462*, 510–513. https://doi.org/10.1038/nature08511.
17. Shin, H., Kumamoto, Y., Gopinath, S., and Iwasaki, A. (2016). CD301b+ dendritic cells stimulate tissue-resident memory CD8+ T cells to protect against genital HSV-2. Nat. Commun. *7*, 13346. https://doi.org/10.1038/ncomms13346.
18. Cunningham, A.L., Nelson, P.A., Fathman, C.G., and Merigan, T.C. (1985). Interferon gamma production by herpes simplex virus antigen-specific T cell clones from patients with recurrent herpes labialis. J. Gen. Virol. *66*, 249–258. https://doi.org/10.1099/0022-1317-66-2-249.
19. Peng, T., Zhu, J., Phasouk, K., Koelle, D.M., Wald, A., and Corey, L. (2012). An effector phenotype of CD8+ T cells at the junction epithelium during clinical quiescence of herpes simplex virus 2 infection. J. Virol. *86*, 10587–10596. https://doi.org/10.1128/JVI.01237-12.
20. Schiffer, J.T., Swan, D.A., Roychoudhury, P., Lund, J.M., Prlic, M., Zhu, J., Wald, A., and Corey, L. (2018). A fixed spatial structure of CD8+ T cells in tissue during chronic HSV-2 infection. J. Immunol. *201*, 1522–1535. https://doi.org/10.4049/jimmunol.1800471.
21. Schiffer, J.T., and Corey, L. (2013). Rapid host immune response and viral dynamics in herpes simplex virus-2 infection. Nat. Med. *19*, 280–290. https://doi.org/10.1038/nm.3103.
22. Zhu, J., Hladik, F., Woodward, A., Klock, A., Peng, T., Johnston, C., Remington, M., Magaret, A., Koelle, D.M., Wald, A., and Corey, L. (2009). Persistence of HIV-1 receptor–positive cells after HSV-2 reactivation is a potential mechanism for increased HIV-1 acquisition. Nat. Med. *15*, 886–892. https://doi.org/10.1038/nm.2006.
23. Zhu, J., Peng, T., Johnston, C., Phasouk, K., Kask, A.S., Klock, A., Jin, L., Diem, K., Koelle, D.M., Wald, A., et al. (2013). Immune surveillance by CD8αα+ skin-resident T cells in human herpes virus infection. Nature *497*, 494–497. https://doi.org/10.1038/nature12110.
24. Harandi, A.M., Svennerholm, B., Holmgren, J., and Eriksson, K. (2001). Interleukin-12 (IL-12) and IL-18 are important in innate defense against genital herpes simplex virus type 2 infection in mice but are not required for the development of acquired gamma interferon-mediated protective immunity. J. Virol. *75*, 6705–6709. https://doi.org/10.1128/JVI.75.14.6705-6709.2001.
25. Lebratti, T., Lim, Y.S., Cofie, A., Andhey, P., Jiang, X., Scott, J., Fabbrizi, M.R., Ozantürk, A.N., Pham, C., Clemens, R., et al. (2021). A sustained type I IFN-neutrophil-IL-18 axis drives pathology during mucosal viral infection. Elife *10*, e65762. https://doi.org/10.7554/eLife.65762.
26. Fehniger, T.A., Cai, S.F., Cao, X., Bredemeyer, A.J., Presti, R.M., French, A.R., and Ley, T.J. (2007). Acquisition of murine NK cell cytotoxicity requires the translation of a pre-existing pool of granzyme B and perforin mRNAs. Immunity *26*, 798–811. https://doi.org/10.1016/j.immuni.2007.04.010.
27. Hyodo, Y., Matsui, K., Hayashi, N., Tsutsui, H., Kashiwamura, S., Yamauchi, H., Hiroishi, K., Takeda, K., Tagawa, Y., Iwakura, Y., et al. (1999). IL-18 up-regulates perforin-mediated NK activity without increasing perforin messenger RNA expression by binding to constitutively expressed IL-18 receptor. J. Immunol. *162*, 1662–1668.
28. Afonina, I.S., Cullen, S.P., and Martin, S.J. (2010). Cytotoxic and non-cytotoxic roles of the CTL/NK protease granzyme B. Immunol. Rev. *235*, 105–116. https://doi.org/10.1111/j.0105-2896.2010.00908.x.
29. Cullen, S.P., and Martin, S.J. (2008). Mechanisms of granule-dependent killing. Cell Death Differ. *15*, 251–262. https://doi.org/10.1038/sj.cdd.4402244.
30. Russell, J.H., and Ley, T.J. (2002). Lymphocyte-mediated cytotoxicity. Annu. Rev. Immunol. *20*, 323–370. https://doi.org/10.1146/annurev.immunol.20.100201.131730.
31. Heusel, J.W., Wesselschmidt, R.L., Shresta, S., Russell, J.H., and Ley, T.J. (1994). Cytotoxic lymphocytes require granzyme B for the rapid induction

of DNA fragmentation and apoptosis in allogeneic target cells. Cell *76*, 977–987. https://doi.org/10.1016/0092-8674(94)90376-x.

32. Shresta, S., MacIvor, D.M., Heusel, J.W., Russell, J.H., and Ley, T.J. (1995). Natural killer and lymphokine-activated killer cells require granzyme B for the rapid induction of apoptosis in susceptible target cells. Proc. Natl. Acad. Sci. USA *92*, 5679–5683. https://doi.org/10.1073/pnas.92.12.5679.

33. Bálint, Š., Müller, S., Fischer, R., Kessler, B.M., Harkiolaki, M., Valitutti, S., and Dustin, M.L. (2020). Supramolecular attack particles are autonomous killing entities released from cytotoxic T cells. Science *368*, 897–901. https://doi.org/10.1126/science.aay9207.

34. Castiblanco, D., Rudd-Schmidt, J.A., Noori, T., Sutton, V.R., Hung, Y.H., Flinsenberg, T.W.H., Hodel, A.W., Young, N.D., Smith, N., Bratkovic, D., et al. (2022). Severely impaired CTL killing is a feature of the neurological disorder Niemann-Pick disease type C1. Blood *139*, 1833–1849. https://doi.org/10.1182/blood.2021013477.

35. Barber, G.N. (2001). Host defense, viruses and apoptosis. Cell Death Differ. *8*, 113–126. https://doi.org/10.1038/sj.cdd.4400823.

36. Froelich, C.J., Dixit, V.M., and Yang, X. (1998). Lymphocyte granule-mediated apoptosis: matters of viral mimicry and deadly proteases. Immunol. Today *19*, 30–36. https://doi.org/10.1016/S0167-5699(97)01184-5.

37. Müllbacher, A., Waring, P., Tha Hla, R., Tran, T., Chin, S., Stehle, T., Museteanu, C., and Simon, M.M. (1999). Granzymes are the essential downstream effector molecules for the control of primary virus infections by cytolytic leukocytes. Proc. Natl. Acad. Sci. USA *96*, 13950–13955.

38. Roychoudhury, P., Swan, D.A., Duke, E., Corey, L., Zhu, J., Davé, V., Spuhler, L.R., Lund, J.M., Prlic, M., and Schiffer, J.T. (2020). Tissue-resident T cell–derived cytokines eliminate herpes simplex virus-2–infected cells. J. Clin. Invest. *130*, 2903–2919. https://doi.org/10.1172/JCI132583.

39. Prakash, M.D., Bird, C.H., and Bird, P.I. (2009). Active and zymogen forms of granzyme B are constitutively released from cytotoxic lymphocytes in the absence of target cell engagement. Immunol. Cell Biol. *87*, 249–254. https://doi.org/10.1038/icb.2008.98.

40. Isaaz, S., Baetz, K., Olsen, K., Podack, E., and Griffiths, G.M. (1995). Serial killing by cytotoxic T lymphocytes: T cell receptor triggers degranulation, re-filling of the lytic granules and secretion of lytic proteins via a non-granule pathway. Eur. J. Immunol. *25*, 1071–1079. https://doi.org/10.1002/eji.1830250432.

41. Jenkins, M.R., Rudd-Schmidt, J.A., Lopez, J.A., Ramsbottom, K.M., Mannering, S.I., Andrews, D.M., Voskoboinik, I., and Trapani, J.A. (2015). Failed CTL/NK cell killing and cytokine hypersecretion are directly linked through prolonged synapse time. J. Exp. Med. *212*, 307–317. https://doi.org/10.1084/jem.20140964.

42. Hiroyasu, S., Zeglinski, M.R., Zhao, H., Pawluk, M.A., Turner, C.T., Kasprick, A., Tateishi, C., Nishie, W., Burleigh, A., Lennox, P.A., et al. (2021). Granzyme B inhibition reduces disease severity in autoimmune blistering diseases. Nat. Commun. *12*, 302. https://doi.org/10.1038/s41467-020-20604-3.

43. Russo, V., Klein, T., Lim, D.J., Solis, N., Machado, Y., Hiroyasu, S., Nabai, L., Shen, Y., Zeglinski, M.R., Zhao, H., et al. (2018). Granzyme B is elevated in autoimmune blistering diseases and cleaves key anchoring proteins of the dermal-epidermal junction. Sci. Rep. *8*, 9690. https://doi.org/10.1038/s41598-018-28070-0.

44. Shen, Y., Zeglinski, M.R., Turner, C.T., Raithatha, S.A., Wu, Z., Russo, V., Oram, C., Hiroyasu, S., Nabai, L., Zhao, H., et al. (2018). Topical small molecule granzyme B inhibitor improves remodeling in a murine model of impaired burn wound healing. Exp. Mol. Med. *50*, 1–11. https://doi.org/10.1038/s12276-018-0095-0.

45. Turner, C.T., Bolsoni, J., Zeglinski, M.R., Zhao, H., Ponomarev, T., Richardson, K., Hiroyasu, S., Schmid, E., Papp, A., and Granville, D.J. (2021). Granzyme B mediates impaired healing of pressure injuries in aged skin. NPJ Aging Mech. Dis. *7*, 6–13. https://doi.org/10.1038/s41514-021-00059-6.

46. Hoshino, K., Tsutsui, H., Kawai, T., Takeda, K., Nakanishi, K., Takeda, Y., and Akira, S. (1999). Cutting edge: generation of IL-18 receptor-deficient mice: evidence for IL-1 receptor-related protein as an essential IL-18 binding receptor. J. Immunol. *162*, 5041–5044.

47. Nakanishi, K. (2018). Unique action of interleukin-18 on T cells and other immune cells. Front. Immunol. *9*, 763.

48. Yoshimoto, T., Takeda, K., Tanaka, T., Ohkusu, K., Kashiwamura, S., Okamura, H., Akira, S., and Nakanishi, K. (1998). IL-12 up-regulates IL-18 receptor expression on T cells, Th1 cells, and B cells: synergism with IL-18 for IFN-γ production. J. Immunol. *161*, 3400–3407.

49. Kaushic, C., Ashkar, A.A., Reid, L.A., and Rosenthal, K.L. (2003). Progesterone increases susceptibility and decreases immune responses to genital herpes infection. J. Virol. *77*, 4558–4565. https://doi.org/10.1128/JVI.77.8.4558-4565.2003.

50. Morrison, L.A., Da Costa, X.J., and Knipe, D.M. (1998). Influence of mucosal and parenteral immunization with a replication-defective mutant of HSV-2 on immune responses and protection from genital challenge. Virology *243*, 178–187. https://doi.org/10.1006/viro.1998.9047.

51. Chetty, A., Darby, M.G., Vornewald, P.M., Martín-Alonso, M., Filz, A., Ritter, M., McSorley, H.J., Masson, L., Smith, K., Brombacher, F., et al. (2021). Il4ra-independent vaginal eosinophil accumulation following helminth infection exacerbates epithelial ulcerative pathology of HSV-2 infection. Cell Host Microbe *29*, 579–593.e5. https://doi.org/10.1016/j.chom.2021.02.004.

52. Khoury-Hanold, W., Yordy, B., Kong, P., Kong, Y., Ge, W., Szigeti-Buck, K., Ralevski, A., Horvath, T.L., and Iwasaki, A. (2016). Viral spread to enteric neurons links genital HSV-1 infection to toxic megacolon and lethality. Cell Host Microbe *19*, 788–799. https://doi.org/10.1016/j.chom.2016.05.008.

53. Parr, M.B., and Parr, E.L. (2003). Intravaginal administration of herpes simplex virus type 2 to mice leads to infection of several neural and extraneural sites. J. Neurovirol. *9*, 594–602. https://doi.org/10.1080/13550280390246499.

54. Pieknik, J.R., Bertke, A.S., and Krause, P.R. (2019). Herpes simplex virus 2 in autonomic ganglia: evidence for spontaneous reactivation. J. Virol. *93*, e00227-19. https://doi.org/10.1128/JVI.00227-19.

55. Pham, C.T., MacIvor, D.M., Hug, B.A., Heusel, J.W., and Ley, T.J. (1996). Long-range disruption of gene expression by a selectable marker cassette. Proc. Natl. Acad. Sci. USA *93*, 13090–13095.

56. Hiebert, P.R., Wu, D., and Granville, D.J. (2013). Granzyme B degrades extracellular matrix and contributes to delayed wound closure in apolipoprotein E knockout mice. Cell Death Differ. *20*, 1404–1414. https://doi.org/10.1038/cdd.2013.96.

57. Jensen, C., Sinkeviciute, D., Madsen, D.H., Önnerfjord, P., Hansen, M., Schmidt, H., Karsdal, M.A., Svane, I.M., and Willumsen, N. (2020). Granzyme B degraded type IV collagen products in serum identify melanoma patients responding to immune checkpoint blockade. Cancers *12*, 2786. https://doi.org/10.3390/cancers12102786.

58. Giudice, G.J., Emery, D.J., and Diaz, L.A. (1992). Cloning and primary structural analysis of the bullous pemphigoid autoantigen BP180. J. Invest. Dermatol. *99*, 243–250. https://doi.org/10.1111/1523-1747.ep12616580.

59. Omoto, Y., Yamanaka, K., Tokime, K., Kitano, S., Kakeda, M., Akeda, T., Kurokawa, I., Gabazza, E.C., Tsutsui, H., Katayama, N., et al. (2010). Granzyme B is a novel interleukin-18 converting enzyme. J. Dermatol. Sci. *59*, 129–135. https://doi.org/10.1016/j.jdermsci.2010.05.004.

60. Voskoboinik, I., Whisstock, J.C., and Trapani, J.A. (2015). Perforin and granzymes: function, dysfunction and human pathology. Nat. Rev. Immunol. *15*, 388–400. https://doi.org/10.1038/nri3839.

61. Barr, D.P., Belz, G.T., Reading, P.C., Wojtasiak, M., Whitney, P.G., Heath, W.R., Carbone, F.R., and Brooks, A.G. (2007). A role for plasmacytoid dendritic cells in the rapid IL-18-dependent activation of NK cells following

HSV-1 infection. Eur. J. Immunol. *37*, 1334–1342. https://doi.org/10.1002/eji.200636362.

62. Fujioka, N., Akazawa, R., Ohashi, K., Fujii, M., Ikeda, M., and Kurimoto, M. (1999). Interleukin-18 protects mice against acute herpes simplex virus type 1 infection. J. Virol. *73*, 2401–2409.
63. Gill, N., Chenoweth, M.J., Verdu, E.F., and Ashkar, A.A. (2011). NK cells require type I IFN receptor for antiviral responses during genital HSV-2 infection. Cell. Immunol. *269*, 29–37. https://doi.org/10.1016/j.cellimm.2011.03.007.
64. Reading, P.C., Whitney, P.G., Barr, D.P., Wojtasiak, M., Mintern, J.D., Waithman, J., and Brooks, A.G. (2007). IL-18, but not IL-12, regulates NK cell activity following intranasal herpes simplex virus type 1 infection. J. Immunol. *179*, 3214–3221. https://doi.org/10.4049/jimmunol.179.5.3214.
65. Varanasi, S.K., Rajasagi, N.K., Jaggi, U., and Rouse, B.T. (2018). Role of IL-18 induced Amphiregulin expression on virus induced ocular lesions. Mucosal Immunol. *11*, 1705–1715. https://doi.org/10.1038/s41385-018-0058-8.
66. Parr, M.B., and Parr, E.L. (2003). Vaginal immunity in the HSV-2 mouse model. Int. Rev. Immunol. *22*, 43–63. https://doi.org/10.1080/08830180305228.
67. Reinert, L.S., Harder, L., Holm, C.K., Iversen, M.B., Horan, K.A., Dagnæs-Hansen, F., Ulhøi, B.P., Holm, T.H., Mogensen, T.H., Owens, T., et al. (2012). TLR3 deficiency renders astrocytes permissive to herpes simplex virus infection and facilitates establishment of CNS infection in mice. J. Clin. Invest. *122*, 1368–1376. https://doi.org/10.1172/JCI60893.
68. Chiang, H.-Y., Lu, H.-H., Sudhakar, J.N., Chen, Y.-W., Shih, N.-S., Weng, Y.-T., and Shui, J.-W. (2022). IL-22 initiates an IL-18-dependent epithelial response circuit to enforce intestinal host defence. Nat. Commun. *13*, 874. https://doi.org/10.1038/s41467-022-28478-3.
69. Jarret, A., Jackson, R., Duizer, C., Healy, M.E., Zhao, J., Rone, J.M., Bielecki, P., Sefik, E., Roulis, M., Rice, T., et al. (2020). Enteric nervous system-derived IL-18 orchestrates mucosal barrier immunity. Cell *180*, 50–63.e12. https://doi.org/10.1016/j.cell.2019.12.016.
70. Hernandez-Pigeon, H., Jean, C., Charruyer, A., Haure, M.-J., Titeux, M., Tonasso, L., Quillet-Mary, A., Baudouin, C., Charveron, M., and Laurent, G. (2006). Human keratinocytes acquire cellular cytotoxicity under UV-B irradiation. Implication of granzyme B and perforin. J. Biol. Chem. *281*, 13525–13532. https://doi.org/10.1074/jbc.M512694200.
71. Hernandez-Pigeon, H., Jean, C., Charruyer, A., Haure, M.J., Baudouin, C., Charvéron, M., Quillet-Mary, A., and Laurent, G. (2007). UVA induces granzyme B in human keratinocytes through MIF. J. Biol. Chem. *282*, 8157–8164. https://doi.org/10.1074/jbc.M607436200.
72. Shin, H., and Iwasaki, A. (2013). Generating protective immunity against genital herpes. Trends Immunol. *34*, 487–494. https://doi.org/10.1016/j.it.2013.08.001.
73. Campos, T.M., Novais, F.O., Saldanha, M., Costa, R., Lordelo, M., Celestino, D., Sampaio, C., Tavares, N., Arruda, S., Machado, P., et al. (2020). Granzyme B produced by natural killer cells enhances inflammatory response and contributes to the immunopathology of cutaneous leishmaniasis. J. Infect. Dis. *221*, 973–982. https://doi.org/10.1093/infdis/jiz538.
74. Novais, F.O., Nguyen, B.T., and Scott, P. (2021). Granzyme B inhibition by tofacitinib blocks the pathology induced by CD8 T cells in cutaneous leishmaniasis. J. Invest. Dermatol. *141*, 575–585. https://doi.org/10.1016/j.jid.2020.07.011.
75. Boivin, W.A., Shackleford, M., Vanden Hoek, A., Zhao, H., Hackett, T.L., Knight, D.A., and Granville, D.J. (2012). Granzyme B cleaves decorin, biglycan and soluble betaglycan, releasing active transforming growth factor-β1. PLoS One *7*, e33163. https://doi.org/10.1371/journal.pone.0033163.
76. Chang, E., Galle, L., Maggs, D., Estes, D.M., and Mitchell, W.J. (2000). Pathogenesis of herpes simplex virus type 1-induced corneal inflammation in perforin-deficient mice. J. Virol. *74*, 11832–11840. https://doi.org/10.1128/jvi.74.24.11832-11840.2000.
77. Simon, M.M., Hausmann, M., Tran, T., Ebnet, K., Tschopp, J., ThaHla, R., and Müllbacher, A. (1997). In vitro– and ex vivo–derived cytolytic leukocytes from granzyme A × B double knockout mice are defective in granule-mediated apoptosis but not lysis of target cells. J. Exp. Med. *186*, 1781–1786. https://doi.org/10.1084/jem.186.10.1781.
78. Dobbs, M.E., Strasser, J.E., Chu, C.F., Chalk, C., and Milligan, G.N. (2005). Clearance of herpes simplex virus type 2 by CD8+ T cells requires gamma interferon and either perforin- or fas-mediated cytolytic mechanisms. J. Virol. *79*, 14546–14554. https://doi.org/10.1128/JVI.79.23.14546-14554.2005.
79. van Dommelen, S.L.H., Sumaria, N., Schreiber, R.D., Scalzo, A.A., Smyth, M.J., and Degli-Esposti, M.A. (2006). Perforin and granzymes have distinct roles in defensive immunity and immunopathology. Immunity *25*, 835–848. https://doi.org/10.1016/j.immuni.2006.09.010.
80. Shrestha, B., Samuel, M.A., and Diamond, M.S. (2006). CD8+ T cells require perforin to clear west nile virus from infected neurons. J. Virol. *80*, 119–129. https://doi.org/10.1128/JVI.80.1.119-129.2006.
81. Andrade, F., Fellows, E., Jenne, D.E., Rosen, A., and Young, C.S.H. (2007). Granzyme H destroys the function of critical adenoviral proteins required for viral DNA replication and granzyme B inhibition. EMBO J. *26*, 2148–2157. https://doi.org/10.1038/sj.emboj.7601650.
82. de Jong, L.C., Crnko, S., Ten Broeke, T., and Bovenschen, N. (2021). Non-cytotoxic functions of killer cell granzymes in viral infections. PLoS Pathog. *17*, e1009818. https://doi.org/10.1371/journal.ppat.1009818.
83. Pardo, J., Balkow, S., Anel, A., and Simon, M.M. (2002). The differential contribution of granzyme A and granzyme B in cytotoxic T lymphocyte-mediated apoptosis is determined by the quality of target cells. Eur. J. Immunol. *32*, 1980–1985. https://doi.org/10.1002/1521-4141(200207)32:7<1980::AID-IMMU1980>3.0.CO;2-Z.
84. Chen, P.-K., Lan, J.-L., Huang, P.-H., Hsu, J.-L., Chang, C.-K., Tien, N., Lin, H.-J., and Chen, D.-Y. (2021). Interleukin-18 is a potential biomarker to discriminate active adult-onset still's disease from COVID-19. Front. Immunol. *12*, 719544.
85. Satış, H., Özger, H.S., Aysert Yıldız, P., Hızel, K., Gulbahar, Ö., Erbaş, G., Aygencel, G., Guzel Tunccan, O., Öztürk, M.A., Dizbay, M., and Tufan, A. (2021). Prognostic value of interleukin-18 and its association with other inflammatory markers and disease severity in COVID-19. Cytokine *137*, 155302. https://doi.org/10.1016/j.cyto.2020.155302.
86. Tjan, L.H., Furukawa, K., Nagano, T., Kiriu, T., Nishimura, M., Arii, J., Hino, Y., Iwata, S., Nishimura, Y., and Mori, Y. (2021). Early differences in cytokine production by severity of coronavirus disease 2019. J. Infect. Dis. *223*, 1145–1149. https://doi.org/10.1093/infdis/jiab005.
87. Kang, C.K., Han, G.-C., Kim, M., Kim, G., Shin, H.M., Song, K.-H., Choe, P.G., Park, W.B., Kim, E.S., Kim, H.B., et al. (2020). Aberrant hyperactivation of cytotoxic T-cell as a potential determinant of COVID-19 severity. Int. J. Infect. Dis. *97*, 313–321. https://doi.org/10.1016/j.ijid.2020.05.106.
88. Mitsuyama, Y., Yamakawa, K., Kayano, K., Maruyama, M., Wada, T., and Fujimi, S. (2021). Prolonged enhancement of cytotoxic T lymphocytes in the post-recovery state of severe COVID-19. J. Intensive Care *9*, 76. https://doi.org/10.1186/s40560-021-00591-3.
89. Zenarruzabeitia, O., Astarloa-Pando, G., Terrén, I., Orrantia, A., Pérez-Garay, R., Seijas-Betolaza, I., Nieto-Arana, J., Imaz-Ayo, N., Pérez-Fernández, S., Arana-Arri, E., and Borrego, F. (2021). T cell activation, highly armed cytotoxic cells and a shift in monocytes CD300 receptors expression is characteristic of patients with severe COVID-19. Front. Immunol. *12*, 655934.
90. Spang, A.E., Godowski, P.J., and Knipe, D.M. (1983). Characterization of herpes simplex virus 2 temperature-sensitive mutants whose lesions map

in or near the coding sequences for the major DNA-binding protein. J. Virol. *45*, 332–342. https://doi.org/10.1128/jvi.45.1.332-342.1983.

91. Narni-Mancinelli, E., Chaix, J., Fenis, A., Kerdiles, Y.M., Yessaad, N., Reynders, A., Gregoire, C., Luche, H., Ugolini, S., Tomasello, E., et al. (2011). Fate mapping analysis of lymphoid cells expressing the NKp46 cell surface receptor. Proc. Natl. Acad. Sci. USA *108*, 18324–18329. https://doi.org/10.1073/pnas.1112064108.

92. Nowarski, R., Jackson, R., Gagliani, N., de Zoete, M.R., Palm, N.W., Bailis, W., Low, J.S., Harman, C.C.D., Graham, M., Elinav, E., and Flavell, R.A. (2015). Epithelial IL-18 equilibrium controls barrier function in colitis. Cell *163*, 1444–1456. https://doi.org/10.1016/j.cell.2015.10.072.

93. Council, N.R. (2011). Guide for the Care and Use of Laboratory Animals, Eighth Edition (The National Academies Press). https://doi.org/10.17226/12910.

94. Lee, A.G., Scott, J.M., Fabbrizi, M.R., Jiang, X., Sojka, D.K., Miller, M.J., Baldridge, M.T., Yokoyama, W.M., and Shin, H. (2020). T cell response kinetics determines neuroinfection outcomes during murine HSV infection. JCI Insight *5*, e134258. https://doi.org/10.1172/jci.insight.134258.

STAR★METHODS

KEY RESOURCES TABLE

REAGENT or RESOURCE	SOURCE	IDENTIFIER
Antibodies		
anti-mouse IL-18 (YIGIF74-1G7)	BioXCell	Cat# BE0237; RRID:AB_2687719
Rat IgG2a (2A3)	BioXCell	Cat# BE0089; RRID:AB_1107769
FITC anti-mouse CD3ε (145-2C11)	Biolegend	Cat# 100306; RRID:AB_312671
PerCP/Cyanine5.5 anti-mouse CD4 (RM4-4)	Biolegend	Cat# 116012; RRID:AB_2563023
Pacific Blue anti-mouse Ly-6G (1A8)	Biolegend	Cat# 127611; RRID:AB_1877212
PE anti-mouse NK-1.1 (PK136)	Biolegend	Cat# 108707; RRID:AB_313394
PE/Dazzle 594 anti-mouse NKp46 (29A1.4)	Biolegend	Cat# 137629; RRID:AB_2616665
PE/Cyanine7 anti-mouse CD8a (53-6.7)	Biolegend	Cat# 100722; RRID:AB_312761
PE anti-mouse CD218a (IL-18Rα) (A17071D)	Biolegend	Cat# 157903; RRID:AB_2860732
PE Rat IgG2b, κ Isotype Ctrl (RTK4530)	Biolegend	Cat# 400607; RRID:AB_326551
APC anti-mouse CD8a (53-6.7)	Biolegend	Cat# 100712; RRID:AB_312751
Alexa Fluor 700 anti-mouse NK-1.1 (PK136)	Biolegend	Cat# 108730; RRID:AB_2291262
PE anti-mouse CD4 (GK1.5)	Biolegend	Cat# 100408; RRID:AB_312693
PerCP/Cyanine5.5 anti-mouse Ly-6G (1A8)	Biolegend	Cat# 127616; RRID:AB_1877271
FITC anti-mouse CD8a (53-6.7)	Biolegend	Cat# 100706; RRID:AB_312745
PE/Dazzle 594 anti-mouse CD4 (GK1.5)	Biolegend	Cat# 100456; RRID:AB_2565845
PE anti-mouse CD3ε (145-2C11)	Biolegend	Cat# 100308; RRID:AB_312673
APC anti-granzyme B (GB12)	ThermoFisher Scientific	Cat# MHGB05; RRID:AB_10373420
anti-mouse CD16/32 (Fc block)	Biolegend	Cat# 101320; RRID:AB_1574975
Live/Dead Fixable Aqua Dead Cell Stain kit	Molecular Probes	Cat# L34957
rabbit anti-HSV primary antibody	Dako	Cat# B0116, RRID:AB_2335703
biotinylated anti-mouse granzyme b antibody (AF1865)	R&D	Cat# BAF1865; RRID:AB_2114416
Rabbit recombinant monoclonal COL17A1 antibody (SR46-05)	Invitrogen	Cat# MA5-31984; RRID:AB_2809278
Goat Polyclonal Anti-Rabbit IgG H&L (Alexa Fluor 488)	Life Technologies	Cat# ab150077, RRID:AB_2630356
Goat Polyclonal anti-Rat IgG H&L (Alexa Fluor 568)	Life Technologies	Cat# A-11077, RRID:AB_2534121
human serum IgG	Innovative Research	Cat# 50643486
Bacterial and virus strains		
HSV-2 186 syn+	Spang et al.[90]	N/A
Chemicals, peptides, and recombinant proteins		
Formaldehyde, Para	Fisher Chemical	Cat# 04042-500
sodium azide	Sigma-Aldrich	Cat# S2002-25G
dry milk	Carnation	N/A
calcium chloride dihydrate	Amresco	Cat# 0556-500G
magnesium chloride hexahydrate	Sigma-Aldrich	Cat# M9272-500G
Triton™ X-100	Sigma-Aldrich	Cat# 93443-100ML
TWEEN® 20	Sigma-Aldrich	Cat# P7949-500ML
2-Mercaptoethanol	Sigma-Aldrich	Cat# M3148-100ML
L-Lysine monohydrochloride	Sigma-Aldrich	Cat# L8662-100G
sodium phosphate monobasic monohydrate	Sigma-Aldrich	Cat# S9638-500G
D-(+)-Glucose	Sigma-Aldrich	Cat# G5767-500G
Sucrose	Sigma-Aldrich	Cat# S0389-500G
Cytofix/Cytoperm Fixation/Permeabilization Solution	BD	Cat# 554722

(*Continued on next page*)

Continued

REAGENT or RESOURCE	SOURCE	IDENTIFIER
Perm/ Wash Buffer	BD	Cat# 554723
Scigen Tissue-Plus™ O.C.T. Compound	Fisher Scientific	Cat# 23-730-571
4′,6-diamidino-2-phenylindole	Life Technologies	Cat# D1306
MedroxyPROGESTERone Acetate	Northstar	NDC 16714-981-01
VTI-1002	ViDA Therapeutics, Provided by D.J. Granville; Shen et al.[44]	N/A
Blank gel (control for VTI-1002)	Provided by D.J. Granville; Shen et al.[44]	N/A
Dispase II	Roche	Cat# 4942078001
Collagenase D	Roche	Cat# 11088866001
Dnase I	Roche	Cat# 10104159001
fetal bovine serum	Corning	Cat# 35-010-CV
DMEM, high glucose	Gibco	Cat# 11965-092
RPMI 1640	Gibco	Cat# 11875-093
Dulbecco′s Phosphate Buffered Saline (DPBS)	Sigma-Aldrich	Cat# D8537-500ML
Phosphate Buffered Saline Powder	Sigma-Aldrich	Cat# P3813
Penicillin-Streptomycin	Gibco	Cat# 15140-122
bovine serum albumin	Sigma-Aldrich	Cat# A9418-10G
normal goat serum	Jackson Immunoresearch	Cat# 005-000-121 RRID: AB_2336990
Normal donkey serum	Jackson Immunoresearch	Cat# 017-000-121 RRID: AB_2337258
Critical commercial assays		
Mouse Granzyme B DuoSet ELISA kit	R&D	Cat# DY1865-05
Mouse IFN-γ DuoSet ELISA kit	R&D	Cat# DY485-05
Mouse IL-18 ELISA kit	MBL	Cat# 7625
Avidin/ Biotin Blocking Kit	Vector Laboratories	Cat# SP-2001 RRID:AB_2336231
Human Granzyme B DuoSet ELISA kit	R&D	Cat# DY2906-05 RRID:AB_2893368
Human Total IL-18 DuoSet ELISA kit	R&D	Cat# DY318-05
Experimental models: Cell lines		
Vero Cells (CCL81)	ATCC	CCL-81; RRID: CVCL_0059
Experimental models: Organisms/strains		
Mouse: C57BL/6J	Jackson Laboratory	Cat# 000664; RRID: IMSR_JAX:000664
Mouse: B6.Cg-Tg(*Cd4-cre*)1Cwi/BfluJ	Jackson Laboratory	Cat# 022071; RRID:IMSR_JAX:022071
Mouse: *Ncr1-Cre*	Provided by W. Yokoyama; Narni-Mancinelli et al.[91]	N/A
Mouse: *Il-18r1*$^{flox/flox}$	Provided by R. A. Flavell; Nowarski et al.[92]	N/A
Mouse: B6.129S2-*Gzmb*tm1Ley/J	Provided by T. J. Ley; Pham et al.[55]	RRID:IMSR_JAX:002248
Mouse: C57BL/6-*Prf1*tm1Sdz/J	Jackson Laboratory	Cat# 002407; RRID:IMSR_JAX:002407
Software and algorithms		
Image J Fiji	NIH	https://imagej.net/software/fiji/
NDP 2.0	Hamamatsu	https://www.hamamatsu.com/jp/en/product/life-science-and-medical-systems/digital-slide-scanner/U12388-01.html
GraphPad Prism	GraphPad Software	http://www.graphpad.com/scientific-software/prism/
FlowJo	BD	https://www.flowjo.com/solutions/flowjo

RESOURCE AVAILABILITY

Lead contact

Further information and requests for resources and reagents should be directed to and will be fulfilled by the lead contact, Haina Shin (haina.shin@wustl.edu).

Materials availability

This study did not generate new unique reagents.

Data and code availability

- All data reported in this paper will be shared by the lead contact upon request.
- This paper does not report original code.
- Any additional information required to reanalyze the data reported in this paper is available from the lead contact upon request.

EXPERIMENTAL MODEL AND SUBJECT DETAILS

Ethics statement

This study was carried out in accordance with the recommendations in the Guide for the Care and Use of Laboratory Animals.[93] The protocols were approved by the IACUC at the Washington University School of Medicine (assurance no. A3381-01). All experiments conducted conformed to the relevant regulatory standards and all efforts were made to minimize animal suffering. All animal experiments were performed under biosafety level 2 (BSL2) containment.

Mice

Six-week-old female C57BL/6J mice were purchased from Jackson Laboratories and rested for at least 1 week and infected at a minimum of 7 weeks of age. *Cd4*-Cre (B6.Cg-Tg(*Cd4*-cre)1Cwi/BfluJ) and *Prf1* KO mice (C57BL/6-*Prf1*tm1Sdz/J) were purchased from Jackson Laboratories. *Ncr1*-Cre mice were provided by W. M. Yokoyama (Washington University, St Louis) and generated as previously described. *Il18r1*$^{fl/fl}$ mice were obtained from R. A. Flavell (Yale University, New Haven).[92] *Gzmb* KO mice were provided by T.J. Ley (Washington University, St. Louis).[55] Cre-littermates generated from breeding pairs were used as controls. All mice used in the study were maintained on a 12 hr light/dark cycle with unlimited access to food and water. This study was carried out in accordance with the recommendations in the Guide for the Care and Use of Laboratory Animals of the National Institutes of Health.

Human samples

De-identified runoff swab samples were acquired from the Clinical Microbiology Laboratory at Barnes Jewish Hospital (St. Louis, MO) on a fee-per-sample basis. Swabs were originally collected from patients with ulcerative pathology of unknown etiology that were tested for the presence of HSV via polymerase chain reaction (PCR) for diagnostic purposes as part of standard care. No limitations were placed on analyzed samples in terms of patient demographics, affected body area, status of other infections, or positive diagnosis of a specific HSV type.

Cell lines

Vero Cells (African green monkey kidney epithelial cells, ATCC) were cultured in Dulbeco's Modified Eagle Medium (Gibco) containing 1% fetal bovine serum (FBS, Corning) and maintained at 37°C with 5% CO_2. All tissue culture experiments were performed under BSL2 containment.

Viruses and virus propagation

WT HSV-2 186 syn+[90] was propagated and titered on Vero cells as previously described. Briefly, to propagate virus stocks, Vero cells were plated in T150 tissue culture flasks. At 80% confluence, the virus was inoculated at 0.01 MOI for incubation at 37°C. At 2–3 days after infection, infected cells were harvested and resuspended in equal volumes of virus supernatant and twice-autoclaved milk prior to sonication. The lysed cells were aliquoted for use as viral stock.

Mouse infection studies

All mice were injected subcutaneously in the neck ruff once with 2 mg of DMPA (Northstar) 5–7 days prior to virus inoculation. For intravaginal virus inoculation, a sterile calginate swab (McKesson) moistened with sterile PBS was used to gently disrupt mucous from the vaginal cavity. Stock virus was diluted in sterile PBS and 5000 PFU virus was inoculated in a 10 μl volume into the vaginal cavity via a pipette tip. For experiments in which IL-18 was neutralized, mice were treated daily with 100 μg of anti-IL-18 antibody (clone YIGIF74-1G7) or rat IgG2a isotype control (clone 2A3) (BioXCell) at 3–5 d.p.i. through an intravaginal route. For experiments in which the protease activity of granzyme B was inhibited, mice were treated daily with 50uL (3.6mg/mL) of gel-formulated VTI-1002 or vehicle control gel (carbopol, propylene glycol, methyl paraben, and propyl paraben in acetate buffer) at 4–6 d.p.i. through an

intravaginal route. Both VTI-1002 and control gel were gifts from D.J. Granville (The University of British Columbia, Vancouver).[44] Selection of mice for each treatment was random. Mice were weighed and monitored for signs of disease for 1 week following infection in an blinded manner and monitored for survival for 2 weeks. Genital disease was scored as follows: 0 – no inflammation, 1 – mild redness and swelling around the vaginal opening, 2 – fur loss and visible ulceration, 3 – severe ulceration and mild signs of sickness behavior (lack of grooming), 4 –hindlimb paralysis, and 5 – moribund as previously described.[50]

METHOD DETAILS

Vaginal tissue processing

All tissues were harvested from animals sedated with ketamine and xylazine and thoroughly perfused with a minimum of 15 ml of PBS. Vaginas were processed as follows: tissue was cut into pieces and digested for 15 min in a shaking water bath held at 37°C in a 0.5 mg/ml solution of Dispase II (Roche) in PBS. Tissues were then transferred to a solution of 0.5 mg/ml Collagenase D (Roche) and 15 μg/ml DNase I (Roche) in RPMI media (Gibco) supplemented with 10% FBS (Corning) and 1% pen/strep (Gibco) and digested for 25 min in a shaking water bath held at 37°C. 50 μl of sterile EDTA was added to each sample and incubated at 37°C for another 5 min. Tissues were then mechanically disrupted through a 70 um cell strainer into a single-cell suspension using a 3 ml syringe plunger. Tissues were washed with RPMI media with 1% FBS, centrifuged, and resuspended in 200 μl RPMI with 1% FBS and 1% pen/strep.

Virus quantification by plaque assay

For quantification of virus in the vaginal lumen, 50 μl washes with sterile PBS were collected using a pipette and a sterile calcium alginate swab, and diluted in 950 μl of ABC buffer (0.5 mM $CaCl_2$, 0.5 mM $MgCl_2$, 1% glucose, and 1% FBS in sterile PBS). For titration of virus from tissue, the peri-vaginal skin and dorsal root ganglia (DRG) and harvested into pre-weighed tubes and flash frozen on dry ice. ABC buffer was added to weighed tissues prior to bead homogenization and clarification by centrifugation. 10-fold serial dilutions of vaginal washes or tissue homogenate were titered by plaque assays on Vero cells plated in 6-well or 12-well plates[94]. After inoculation and incubation for an hour, overlay media with human IgG was added to each well. Vero cells were stained with 0.1% crystal violet for counting after a 2 day incubation period. All tissue culture experiments were performed under BSL2 containment.

Flow cytometry

Single-cell suspensions were plated in 96-well U-bottom plates and incubated with Live/Dead Fixable Aqua Dead Cell Stain kit (Molecular Probes) for 15 min at room temperature (RT) in the dark and then incubated with TruStain FcX (anti-CD16/32, Biolegend) for 15 min at RT in the dark. Surface staining was performed in FACS buffer (1% FBS and 0.02% sodium azide in PBS) on ice and in the dark using the following antibodies: CD3 (clone 145–2 C11), CD4 (clone GK1.5), CD8a (clone 53–6.7), Ly6G (clone 1A8), NK1.1 (clone PK136), NKp46 (clone 29A1.4), IL-18R1 (clone A17071D). All antibodies were purchased from Biolegend. For intracellular staining, cells were first fixed and permeabilized by cytofix/cytoperm buffer (BD) for 30 min at RT in the dark. Intracellular staining was performed in 1X perm/wash buffer (BD) using anti-Granzyme B (clone GB12, Invitrogen) antibody. Cell counts were performed by adding Precision Count Beads (Biolegend) to samples prior to flow cytometric acquisition. The LSR Fortessa was used for sample acquisition (BD Biosciences) and FlowJo (Treestar) was used for analysis.

Cytokine and granzyme B measurement

To measure mouse cytokine and granzyme B secretion in the vaginal lumen, 2x50 μL washes with sterile PBS were collected using a pipette from each mouse at indicated timepoints after infection. Washes were centrifuged to remove cells and mucus, and supernatants were snap-frozen on dry ice. ELISA kits were used to measure granzyme B, IFNγ (R&D) and IL-18 (MBL) according to the manufacturer's protocol. For human samples, IL-18 and granzyme B were measured in the viral collection media used to collect and store swabs. Commercial ELISA kits for each respective analyte (R&D) were used according to manufacturer's protocol.

Tissue immunohistochemistry and immunofluorescent staining

All tissues were harvested from animals sedated with ketamine and xylazine and thoroughly perfused with a minimum of 15 ml of PBS, followed by 15 ml of 4% PFA for immunohistochemistry (IHC) and immunofluorescent (IF) staining. Tissues were cryoprotected in 30% sucrose, frozen in OCT medium (Fisher Scientific), and cut into 7 um sections onto a polylysine glass slide. For IHC, sections were counterstained with hematoxylin and eosin (H&E), and whole slide images were captured using NanoZoomer 2.0-HT System (Hamamatsu) and analyzed with the NDP.view2 software (Hamamatsu). The length of the entire vaginal epithelium was first traced and determined, followed by areas with epithelial denuding and damage (Figure S2). The percentage of ulcerated epithelium was calculated as damaged vaginal epithelium over total epithelium length[51], areas of epithelial damaged was defined by separation of the epithelium from the lamina propria and exposure of the lamina propria to the lumen due to denuded epithelium. For immunofluorescence, cryosections were first blocked with 5% bovine serum albumin (BSA), 5% goat serum (Jackson Immunoresearch), and 0.1% Triton-X in PBS for 1 hr at RT. Cryosections were then treated with the Avidin/Biotin Blocking Kit (Vector Laboratories) according to manufacturer's protocol. Granzyme B was detected with a biotinylated primary goat anti-mouse polyclonal antibody (AF1865, R&D systems), incubated overnight at 4°C and washed in PBS. Streptavidin-conjugated Alexa Fluor 647 (Life Technologies) was then

added for 30 minutes at RT to visualize granzyme B. Collagen XVII was detected with an primary rabbit anti-mouse monoclonal antibody (SR46-05, Invitrogen), incubated overnight at 4°C and washed in PBS. A secondary goat anti-rabbit Alexa Fluor 568 IgG antibody (Life Technologies) was then added for 30 minutes at RT to visualize collagen XVII. DNA was visualized with 4',6-diamidino-2-phenylindole (DAPI) (Life Technologies). Sections were imaged with a Zeiss Cell Observer inverted microscope using a 40x objective, acquired with Zen software, and total image exposure was adjusted using Photoshop (Adobe). Granzyme B+ cells were quantified using ImageJ Fiji software (NIH) as previously described.[94] Briefly, each image was divided into a grid of 10000 pixels^2 squares (Figure S6). Squares that fell within 30000 pixels^2 (3 squares) of the basement membrane, as denoted by collagen XVII staining were marked, and granzyme B+ cells that fell within the marked squares were considered proximal and counted. Total proximal granzyme B+ cell counts were then divided by total number of squares involved to obtain a frequency of granzyme B+ cells/10000 pixels^2 squares. Image brightness was adjusted using Photoshop (Adobe) and merged with Image J64 (NIH).

QUANTIFICATION AND STATISTICAL ANALYSIS

Statistical analysis

All numerical data analyses were performed on Graphpad Prism 9 software. Values were log-transformed to normalize distribution and variances where necessary. Statistical significance for datasets with more than two variables were analyzed by repeated measures two-way analyses of variance (ANOVA) with Bonferroni's multiple comparisons test. The Geisser-Greenhouse correction was used for ordinal datasets to correct any violations of sphericity and to provide a more stringent calculation of p values. For comparisons between two groups of normally distributed, continuous datasets at a given time point, statistical significance was measured by unpaired two-tailed Student's t-test. Pearson correlation was used to analyze correlations between two continuous datasets. A $p < 0.05$ was considered statistically significant. To maintain objectivity and to remove investigator bias, all data collection, including disease scoring, measurement of epithelial damage, and viral titering, were performed blinded. Where treatment interventions were applicable, mice were treated by one investigator and inflammation was assessed in a blinded manner by another investigator. Experiments were unblinded only after completion of data analysis. No outliers were excluded from our data. No predefined power analyses were performed to determine group sizes to achieve statistical significance; rather, group sizes were determined by historical data generated by our laboratory. To minimize potential confounding effects of microbiome and genetic background, only littermates were used as controls for all mutant mice that were bred in-house. For mutant mice that were purchased, recommended control mice of the same genetic background were purchased from the same vendor. Mouse and sample numbers per group and experimental repeat information is provided in the figure legends. All data points represent individual biological replicates, and the 'n' for each group refers to biological replicates.